Nuclear magnetic resonance, luminescence and structural studies of lanthanide complexes with octadentate macrocyclic ligands bearing benzylphosphinate groups

Silvio Aime,[a] Andrei S. Batsanov,[b] Mauro Botta,[a] Rachel S. Dickins,[b] Stephen Faulkner,[b] Clive E. Foster,[b] Alice Harrison,[c] Judith A. K. Howard,[b] Janet M. Moloney,[b] Timothy J. Norman,[b] David Parker,*,[b] Louise Royle[b,c] and J. A. Gareth Williams[b]

[a] Dipartimento di Chimica Inorganica, Chimica Fisica e Chimica di Materiali, Università di Torino, Via P. Giuria 7-10125 Torino, Italy
[b] Department of Chemistry, University of Durham, South Road, Durham, UK DH1 3LE
[c] MRC Radiobiology Unit, Chilton, Didcot, UK OX11 0RD

The solution and solid-state structures of lanthanide complexes of 1,4,7,10-tetraazacyclododecane-1,4,7,10-tetryltetramethylenetetra(benzylphosphinate), L^{1a}, and of its o-, m- and p-methoxybenzyl analogues (L^2, L^3, L^4) have been investigated by NMR, relaxometry, crystallographic and photophysical methods. It has been shown that the number of proximate water molecules is dependent on the size of the bound lanthanide ion: the complex $[LaL^{1a}]^-$ is nine-co-ordinate and adopts a twisted square-antiprismatic structure with one bound water molecule. The analogous $[YL^{1a}]^-$, $[YbL^{1a}]^-$, $[GdL^{1a}]^-$ and $[EuL^{1a}]^-$ complexes also adopt a twisted square-antiprismatic geometry, but are eight-co-ordinate, with no metal-bound water. Relaxivity studies with the gadolinium complexes showed that they are purely 'outer-sphere' contrast agents, but they associate strongly with proteins leading to a pronounced relaxivity enhancement. Detailed biodistribution studies with $[GdL^{1a}]^-$ revealed avid biliary uptake at low doses and a well defined tendency for the complex to be cleared more slowly from tumour tissue, allowing tissue differentiation.

The solution complexation chemistry of the lanthanides has been the subject of renewed interest over the last few years. As a result of their unique $4f^n$ electronic configurations the lanthanide ions exhibit 'atom-like' spectroscopic and magnetic properties in their complexes, rendering them suitable as probes for time-resolved assays,[1–3] for the labelling of DNA,[4,5] as paramagnetic contrast agents for magnetic resonance imaging (MRI)[6–8] and as shift reagents in NMR spectroscopy.[9,10]

As part of our investigations into kinetically stable lanthanide complexes for MRI and as luminescent probes[11–16] we have been engaged in the development of the complexation chemistry of the octadentate tetrabenzylphosphinate ligand (L^{1a}) which forms kinetically stable complexes with lanthanide ions. The complexes of Y, Eu, Gd and Yb have been assumed to be isostructural, with the lanthanide adopting an eight-co-ordinate structure, with no proximate water molecules.[14,16] In order to define this phenomenon more closely we have prepared a wider range of lanthanide complexes of the tetrabenzyl ligand L^{1a}. We report a variation in complex structure across the series, associated with the lanthanide contraction from the larger lanthanum ion to the smaller, later lanthanides. In addition, the variation in the ^{31}P NMR chemical shift has been measured across the lanthanide series and the results correlated with measurements of related NMR-derived parameters, established in earlier measurements of variations across the lanthanide series.[17]

In order to probe the effect of an aryl substituent on the structure of the lanthanide complexes, a series of methoxy-benzylphosphinate derivatives has also been synthesized, and the properties of selected lanthanide complexes investigated, including the results of relaxivity measurements on gadolinium complexes and photophysical measurements on the related luminescent terbium complexes. Further biodistribution studies have been undertaken with $[GdL^{1a}]^-$, in particular examining the variation of the biodistribution of the complex as a function of the amount of complex given. In addition, the effect of
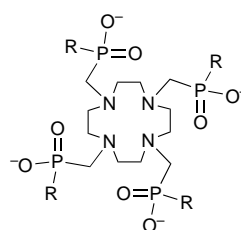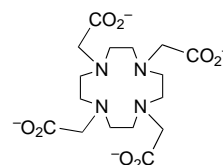

L^{1a} R = PhCH_2
L^{1b} R = Me
L^2 R = 2-MeOC_6H_4CH_2
L^3 R = 3-MeOC_6H_4CH_2
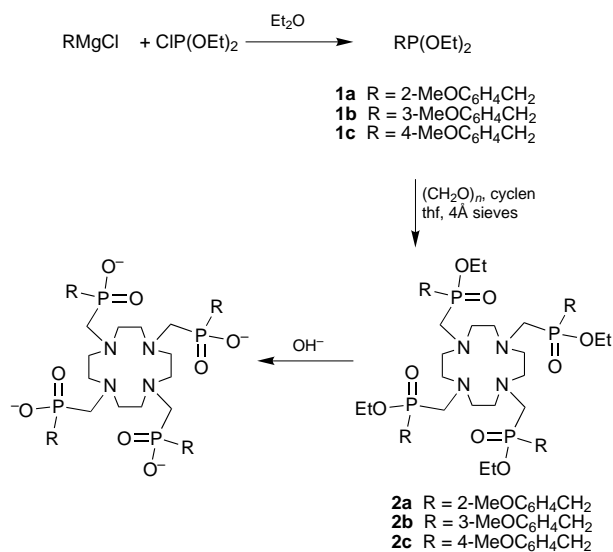L^4 R = 4-MeOC_6H_4CH_2

L^5 (dota)

co-administering a known inhibitor of the 'organic anion transporter' has been examined, in order to characterise the selective biliary clearance of this complex.[12]

Results and Discussion

Synthesis

The absence of a bound water molecule at the binding site of the tetrabenzyl complexes of Y, Eu, Gd and Yb suggested that a study be undertaken of the analogous systems incorporating methoxybenzyl groups in place of the P-benzyl substituents. It was reasoned that the presence of the methoxy group might promote the introduction of a hydrogen-bonded water molecule close to the co-ordinated lanthanide ion. The introduction of such an inner-sphere or 'second-sphere' water molecule could enhance the overall relaxivity of the corresponding gadolinium complex, particularly when bound to a macromolecule.[14]

The series of methoxy-substituted ligands, $L^{2–4}$, was syn-

$$RMgCl \ + \ ClP(OEt)_2 \ \xrightarrow{\ Et_2O\ } \ RP(OEt)_2$$

1a R = 2-MeOC$_6$H$_4$CH$_2$
1b R = 3-MeOC$_6$H$_4$CH$_2$
1c R = 4-MeOC$_6$H$_4$CH$_2$

(CH$_2$O)$_n$, cyclen
thf, 4Å sieves

2a R = 2-MeOC$_6$H$_4$CH$_2$
2b R = 3-MeOC$_6$H$_4$CH$_2$
2c R = 4-MeOC$_6$H$_4$CH$_2$

Scheme 1 thf = Tetrahydrofuran; cyclen = 1,4,7,10-tetraazacyclodo-decane

thesized following the procedures shown in Scheme 1. The intermediate dialkoxyphosphines **1a–1c** were prepared from diethyl chlorophosphite and the appropriate Grignard reagent. The phosphines were used immediately after separation from the magnesium salts, their purity having been confirmed by a combination of ^{31}P and ^{1}H NMR spectroscopy. Co-conden-sation of 1,4,7,10-tetraazacyclododecane with freshly sublimed paraformaldehyde (CH$_2$O)$_n$ in the presence of the appropriate dialkoxyphosphine yielded the intermediate tetra esters **2a–2c** as a mixture of diastereoisomers. Purification was undertaken by chromatography on neutral alumina and subsequent base hydrolysis with aqueous potassium hydroxide was used to furnish the corresponding phosphinic acid salts.[11]

Complexation reactions were carried out in aqueous solution typically by addition of equimolar quantities of the appropriate lanthanide acetate at pH 6 followed by heating at 70 °C for up to 15 h. The lanthanide complexes of the methoxy-substituted ligands were much less soluble than those derived from the parent L^{1a}. Thus while [GdL^{1a}]$^-$ possesses an aqueous solubility of 40 mmol dm^{-3} at room temperature, none of the correspond-ing complexes of L^2, L^3 or L^4 exhibited solubilities in excess of 1 mmol dm^{-3}, limiting their potential in any practical application.

Lanthanum complexes

The ^{31}P NMR spectra of the lanthanum complexes of L^{1a} and L^3 recorded at pD 6 revealed two resonances around δ 38 in relative ratio 8:1. On warming to 80 °C the resonances coalesced (T_c = 328 K, $\Delta G^* = ca.$ 65 kJ mol^{-1}) and this behaviour was reversible over two temperature cycles between 80 and 20 °C. Proton NMR spectra for [LaL^{1a}]$^-$ recorded at 298 K revealed that the broad diastereotopic NCH$_2$P resonances centred at δ 2.52 and 3.61 [assigned with the aid of ^{31}P-decoupled ^{1}H spectra and ^{1}H–^{1}H correlation spectroscopy (COSY) experiments] coalesced on warming to 353 K. The benzylic CH$_2$P protons resonated as a broadened multiplet at 298 K, which sharpened on heating to a well defined doublet ($^2J_{HP}$ = 13 Hz) at 353 K. Within each of the five-membered ring chelates engendered by co-ordination of the La to the four nitrogens of the macrocyclic ring the 'axial' and 'equatorial' protons resonated as four sets of resonances consistent with time-averaged C_4 symmetry for this complex. The resonances due to the 'equatorial' protons appeared as broadened doublets at δ 2.12 and 2.33 while the 'axial' protons were observed to higher frequency as broadened triplets centred at δ 3.5 and 3.6. In the room-temperature ^{13}C NMR spectrum of [LaL^1]$^-$ two

distinct resonances were observed for the ring carbons, one of which was coupled to phosphorus ($^3J_{CP}$ = 12 Hz). Similar behaviour, which is consistent with a locally C_4 symmetric twelve-membered ring that is not inverting rapidly on the NMR time-scale, has been seen in analogous C_3-symmetric hexaden-tate triphosphinate complexes (*e.g.* of Ga^{3+}) based on triaza-cyclononane. The ring carbon which is coupled to phosphorus (δ$_C$ 54.6) possesses a P–C–N–C dihedral angle of close to 180° giving rise to a significant three-bond coupling, whereas the other carbon (δ$_C$ 56.7) defines a P–C–N–C dihedral angle of approximately 90° and the coupling constant is too small to be resolved.[18]

The proton and ^{31}P NMR spectra of the [LaL^3]$^-$ complex were very similar in nature to those of [LaL^{1a}]$^-$. This pattern of behaviour is similar to that observed with complexes of [YL^{1a}]$^-$, where one dominant diastereoisomer was observed (ratio >10:1) by NMR spectroscopy which did not undergo signifi-cant exchange broadening in the temperature range 20 to 70 °C.[14] The main differences were in the proton NMR spectra. For example, with the yttrium complex, the chemical shift non-equivalence of the diastereotopic benzylic CH$_2$P protons was 0.6 ppm, whereas with the lanthanum complex it was less than 0.1 ppm. The non-equivalence in the yttrium complex may be ascribed to the proximity of the pro-S hydrogen to the aniso-tropic phosphorus–oxygen double bond: in the lanthanum complexes the benzylic hydrogens must be oriented differently. The crystallographic analysis of this yttrium complex had earlier established an eight-co-ordinate structure with a twisted square-antiprismatic geometry about the metal centre and a twist angle of 29° for the N$_4$ and O$_4$ planes.[14] The similarity of the ^{31}P shift of the complexes of Y and La (δ 39.4 and 37.6) of L^1 and the observation of one dominant diastereoisomer (*RRRR* or *SSSS* at P) suggested that the two isomers observed in solution with La were associated with a twisted square-antiprismatic (major species) and square-antiprismatic geom-etry about the metal ion.[11,14] Interconversion between these two isomers, observed by NMR on heating, may occur by a co-operative ring inversion or by a sliding motion of the pendant nitrogen substituents about the rigid 12-N$_4$ framework. Such fluxional processes have been identified in explaining the solu-tion dynamics of lanthanide complexes of the related tetra-carboxylate ligand 1,4,7,10-tetraazacyclododecane-1,4,7,10-tetraacetate L^5 (dota).[19]

Using single-crystal X-ray diffraction, full crystal structures were determined for the complexes of Eu and (with lower pre-cision) La and Yb of L^{1a}. Crystal lattice and space groups for the gadolinium complex were also determined (Table 5, Experimental section), proving the similarity of the crystal, and as far as can be seen, of the molecular structures. The euro-pium, gadolinium and ytterbium structures were very similar to those of the yttrium complex which was reported earlier [Figs. 1 and 2(*a*)].[14]

The ligand L^{1a} coordinates the lanthanide ion by four nitro-gens and four phosphinate oxygen atoms, which occupy the vertices of a twisted square prism. The twist around the local four-fold axis [*ca.* 29° in all cases, Fig. 2(*a*)] is intermediate between those in an ideal prism (0°) and an antiprism (45°), but closer to the latter (such an arrangement has been termed an 'inverted square antiprism').[14,15] The antiprism and the dodecahedron are the two principal polyhedra for co-ordination number 8; the former can be converted into the latter by folding both square bases of the antiprism by 29°. There is no evidence for such a conversion in [YL^{1a}]$^-$ and [EuL^{1a}]$^-$, where the N$_4$ and O$_4$ bases of the twisted prism are planar and parallel within experimental error. In [LaL^{1a}(H$_2$O)]$^-$ the metal co-ordination is completed by an aqua ligand, capping the O$_4$ base of the twisted prism. This base remains planar, while the N$_4$ one is folded by 6.5°.

Comparison of the co-ordination polyhedra [Fig. 2(*b*), Table 1] shows that the size of the N$_4$ square remains practically
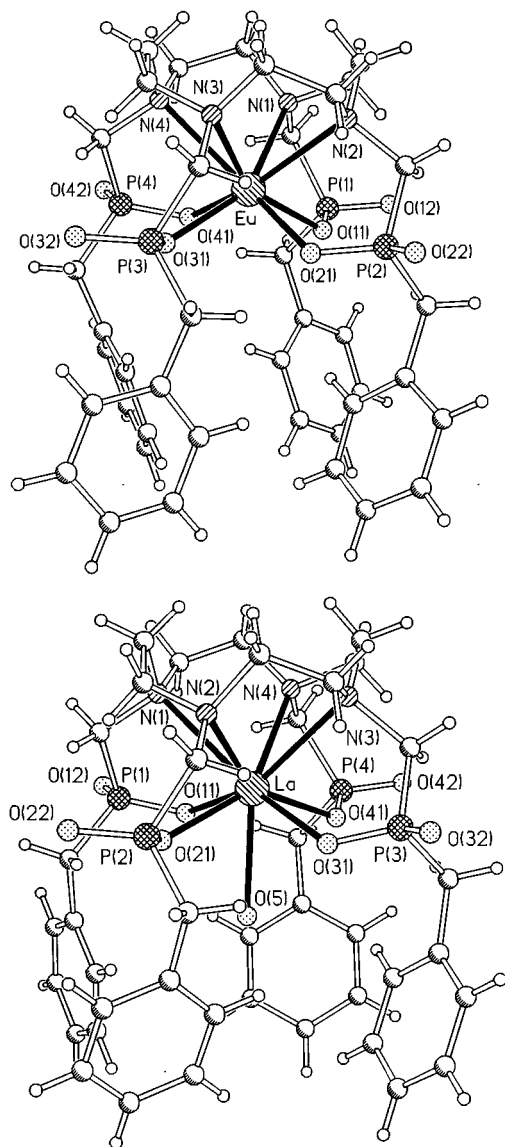
Fig. 1 Structures of the complexes [EuL^{1a}]$^-$ and [LaL^{1a}]$^-$ in the crystal

constant (determined by the favourable square [3.3.3.3] conformation of the 12-N$_4$ ring) and the O$_4$ square is of the same size in [EuL^{1a}]$^-$ and slightly (by *ca.* 0.1 Å in the side) smaller in [YL^{1a}]$^-$. However, the metal atom is not equidistant from the two bases, but is substantially shifted towards the O$_4$ one, the Ln–O bond being up to 0.4 Å shorter than the Ln–N ones. Additional water co-ordination in [LaL^{1a}(H$_2$O)]$^-$ exacerbates this shift, while causing the O$_4$ base to expand; thus the latter complex has wider O–Ln–O and narrower N–Ln–N angles than the eight-co-ordinate ones. The peculiar feature of the Ln–L^{1a} co-ordination is the *cis* orientation of the four benzyl groups which form a hydrophobic mantle around the potential site of water co-ordination, thus making the presence (or absence) of the aqua ligand practically irrelevant to the overall shape of the anion and to intermolecular hydrogen bonding.

The overall local symmetry of the complex anion (both with or without the additional water co-ordination) can be approximated as C_4. The orthorhombic crystal structures of the complexes are characterised by a pseudo-tetragonal lattice with $a \approx b$ (in the monoclinic ytterbium structure all this reasoning is applicable to the pseudo-orthorhombic Niggli cell) and pseudo-tetragonal packing of the anions. However, the pseudo-fourfold *molecular* axes are nearly coincident with the [1 1 0] and [1 $\bar{1}$ 0] directions of the lattice, *i.e.* are perpendicular to the *crystal* pseudo-tetragonal axis *z*. Such packing of the anions leaves the infinite channels in the crystal (*ca.* 7.5 Å in diameter) having

the [0 0 *z*] and [$\frac{1}{2}$ $\frac{1}{2}$ *z*] as their axes. In the studied structures these channels are occupied by water (and/or methanol) molecules of crystallisation, hydrogen bonded to each other and, some of them, to the outward-looking non-co-ordinated phosphate oxygen atoms of the anions (no hydrogen bonds with the co-ordinated water were found). The cations are also located in the channel. As far as the X-ray diffraction evidence goes, the number, positions and even nature of the solvent and cation vary from one complex to another (indeed, may vary for the same complex, depending on the conditions of crystallisation). Thus, in the complexes of Y and La, the cation is a hydrated proton (unobserved in the X-ray experiment), in the europium complex proton and sodium in a 1:1 ratio, and in the ytterbium complex probably potassium. Given the width of the channels, this is not surprising, for even a large moiety (*e.g.* a hydrated alkali-metal ion) has room enough to move along the channel, in accordance with the extreme instability of the crystals outside the mother-liquor (even under an inert atmosphere) and slight but observable variations of unit-cell parameters between crystals of the same complex. Such structure gives ample possibilities for disorder (both static and dynamic) of the channel contents, which was really observed in every structure. Furthermore, with larger counter ions, incommensurate phases can be expected (which may be the case for Yb). The cumulative effect of these factors is to reduce substantially the precision and accuracy of the structure determinations, even more so as the lattice pseudo-symmetry makes the crystals particularly prone to twinning.

Biodistribution studies with [GdL^1]$^-$

The lipophilic anionic complex [GdL^{1a}]$^-$ is attractive for detailed study as a contrast agent for magnetic resonance imaging. It possesses a high kinetic stability with respect to proton-catalysed dissociation[12] {k_{obs} at pH 1 is 24×10^{-6} s^{-1}, *cf.* 1.1×10^{-3} for [Gd(dtpa)]$^{2-}$ [H$_5$dtpa = (carboxymethyl)iminobis(ethylenenitrilo)tetraacetic acid] and 3.2×10^{-6} s^{-1} for [Gd(dota)]$^-$}, and exhibits a high degree of selectivity for clearance *via* the biliary system, rather than the renal route. It possesses a water solubility of 40 mmol dm^{-3}. Previous reports have described the biodistribution of the ^{153}Gd-radiolabelled complexes at a low injected dose (0.01 µmol dm^{-3}).[12] These studies have been extended to include the effect of varying the injected dose from this tracer one (*i.e.* 0.1 µmol dm^{-3}) to a clinical imaging dose (0.1 mmol dm^{-3}). In addition, experiments have been undertaken to confirm that the complex is handled by the 'organic anion transporter', which is known to be inhibited by co-administration of the drug sodium bromosulfophthalein.[20]

Five minutes after injecting a 0.1 µmol dm^{-3} solution of [GdL^{1a}]$^-$ over 14% of the dose is in the liver, with 3% in the gall bladder and 45% in the small intestine. By 2 h (Fig. 3) there was less than 0.005% of the injected dose left in the blood, and only 0.05% of the dose was in the liver. Most of the complex has entered the intestine, and by that time has passed into the caecum and the large intestine. After 24 h most of the complex had left the animal, with only very small amounts left in the elimination pathway. When increasing doses of the complex were administered there were significant differences even after 5 min. The dose dependence was characterised by an increase in the relative amount of complex that was handled by the kidneys, a slower rate of blood clearance and a corresponding decrease in the percentage dose in the gall bladder and small intestine (Fig. 4). The amount of the complex present in the liver after 5 min is the sum of that being cleared by the liver and the blood content of the liver (the liver is 30% perfused by blood). Thus the total amount of complex found in this organ does not vary so markedly as the total dose of complex is increased, dropping from 14 (0.01 µmol dm^{-3}) to 9% (0.1 mmol dm^{-3}).
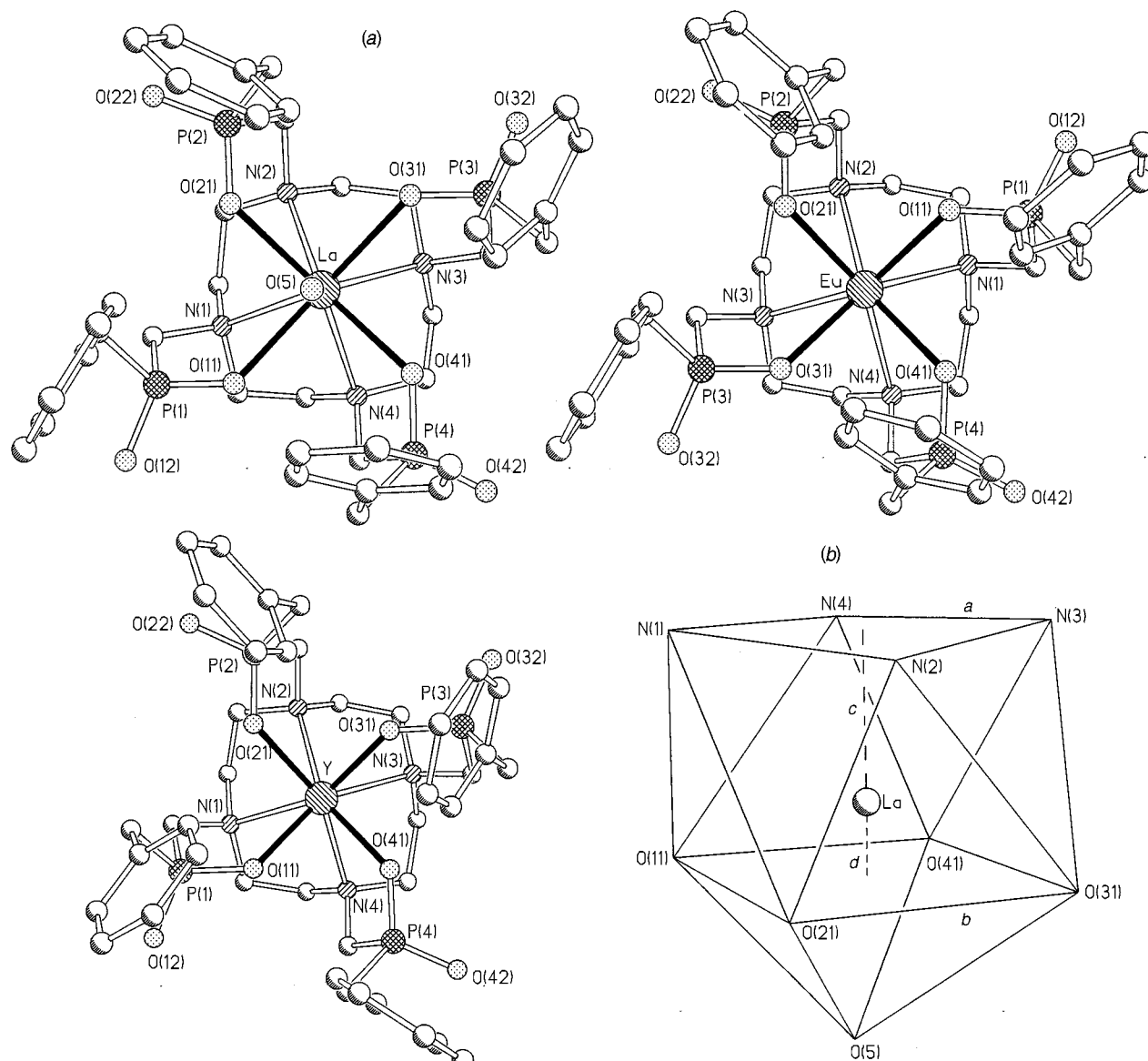
Although there are only very small amounts of the complex

Fig. 2 (*a*) View down the C_4 axis in the structures of the complexes [LaL^{1a}]$^-$, [EuL^{1a}]$^-$ and [YL^{1a}]$^-$. (*b*) Co-ordination polyhedron about the Ln ion: *a* and *b* are the average sides of the N$_4$ and O$_4$ antiprism bases, *c* and *d* the distances (Å) of the lanthanide atom from these bases

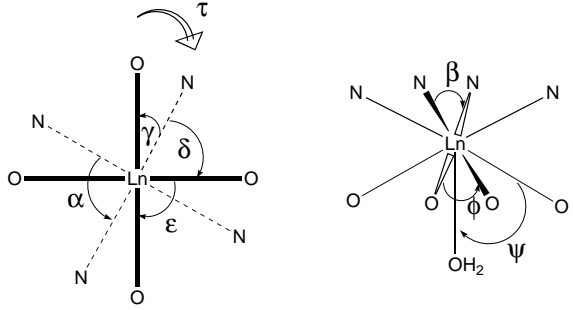| Ln	Y	Eu	La
a	2.97(2)	2.97(1)	2.97(5)
b	2.88(6)	2.99(4)	3.27(3)
c	1.64	1.68	1.85
d	0.97	0.97	0.81

remaining in the excretion pathways after 24 h, it is evident that the larger the dose given the slower is the overall rate of clearance from the body. Comparison has been made between the behaviour of [GdL^{1a}]$^-$, the hydrophilic P-methyl analogue, [GdL^{1b}]$^-$, and [Gd(dtpa)]$^{2-}$, both in terms of the dose-dependent biodistribution and with regard to longer-term retention.[12] The comparative data (Figs. 5 and 6) reveal that 5 min after administration of 0.1 mmol dm^{-3} of complex the amount of [GdL^{1a}]$^-$ in the intestine is still four times greater than for the other two hydrophilic complexes. The amount of complex in the blood and kidneys at this time is similar for all three complexes. After 24 h (Fig. 6) there is still some renal clearance of [GdL^{1a}]$^-$ at the higher dose, as the percentage dose in the kidneys was about seven times that found with the lower dose.

With the analogous gadolinium P-methyl complex, [GdL^{1b}]$^-$ the biodistribution at 5 min at both doses is very similar. By 24 h there is ten times more complex in the gut and three times more in the liver for the 0.1 mmol dm^{-3} dose, *i.e.* there is

a small degree of hepatobiliary excretion at the higher dose. The amount of complex retained in the skeleton is 0.07% from the higher dose after 24 h, and by 7 d this had reduced to 0.03% dose, consistent with the high stability of the complex *in vivo*. It has previously been established that premature decomplexation of Gd from such complexes is characterised by deposition of Gd in the skeleton accompanied by retention in the liver.[12,21]

With [Gd(dtpa)]$^{2-}$ the biodistribution at 5 min was also more or less independent of the dose given. The amount of radiolabel retained in the skeleton and liver at 24 h from the higher dose was 0.11 and 0.15%, compared to 0.30 and 0.65% respectively from the lower dose of this complex. This increased percentage retention in the liver and the skeleton at the lower dose must be related to the established susceptibility of this complex to undergo cation- and/or acid-promoted dissociation, but is difficult to understand.[21] At the lower dose the concentration of complex is low relative to the concentration of cations in the blood (*e.g.* Zn^{2+}) and a higher proportion evidently dissociates than at the higher dose, where the relative concentration of

Table 1 Relevant bond distances (Å) and angles (°) in the complexes

	[YL^{1a}]$^+$	[LaL^{1a}(H$_2$O)]$^+$	[EuL^{1a}]$^+$	[YbL^{1a}]$^+$ *
Ln–N(1)	2.66(2)	2.84(3)	2.68(1)	2.63(1)
Ln–N(2)	2.64(2)	2.69(3)	2.65(1)	2.62(1)
Ln–N(3)	2.67(2)	2.83(2)	2.70(1)	2.62(1)
Ln–N(4)	2.67(2)	2.84(2)	2.72(1)	2.64(1)
average Ln–N	2.667(14)	2.80(6)	2.69(3)	2.63(1)
Ln–O(11)	2.26(2)	2.47(2)	2.349(9)	2.22(1)
Ln–O(21)	2.31(2)	2.42(2)	2.321(8)	2.29(1)
Ln–O(31)	2.20(2)	2.50(2)	2.328(9)	2.23(1)
Ln–O(41)	2.25(2)	2.41(2)	2.304(8)	2.26(1)
average Ln–O (L^{1a})	2.26(4)	2.45(4)	2.326(16)	2.25(3)
Ln–O(w)	—	2.66(2)	—	—
Average angles				
Individual e.s.d.s	0.6–0.7	0.6–0.8	0.3	0.2
N–Ln–N, α	67.7(7)	64(2)	67.1(5)	68.0(3)
N–Ln–N, β	103.5(7)	97(2)	102.9(3)	104.6(2)
N–Ln–O (L^{1a}), γ	69.2(7)	66(2)	69.0(6)	70.4(5)
N–Ln–O (L^{1a}), δ	85.5(6)	83(1)	84.9(1.4)	85.2(4)
O (L^{1a})–Ln–O (L^{1a}), ε	79.3(1.5)	84(1)	80(1)	78.4(5)
O (L^{1a})–Ln–O (L^{1a}), φ	128.9(6)	141(1)	130.8(7)	126.6(2)
O (L^{1a})–Ln–O(w), ψ	—	71(2)	—	—
Antiprism twist, τ	29(1)	28.8(7)	29.5(6)	30.5(5)

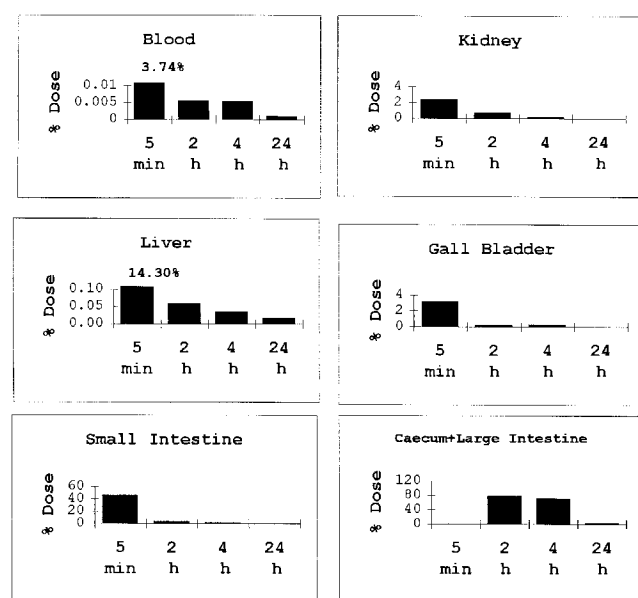* Averaged over two symmetrically independent molecules.

Fig. 3 Biodistribution of [GdL^{1a}]$^-$ in mice at a dose of 0.1 μmol kg^{-1}

[Gd(dtpa)]$^{2-}$ to available endogenous cations is higher. The amount of ^{153}Gd in the skeleton after 7 d is 0.15%, which is a significantly higher figure than that found for the other two complexes. Unlike the situation with the macrocyclic complexes where the percentage dose reduces over 7 d, the % dose in the skeleton remains constant or increases slightly, showing that [Gd(dtpa)]$^{2-}$ is less stable *in vivo* than the other two complexes. This conclusion accords with the relative rates of acid-catalysed dissociation for these complexes referred to above.[12,21]
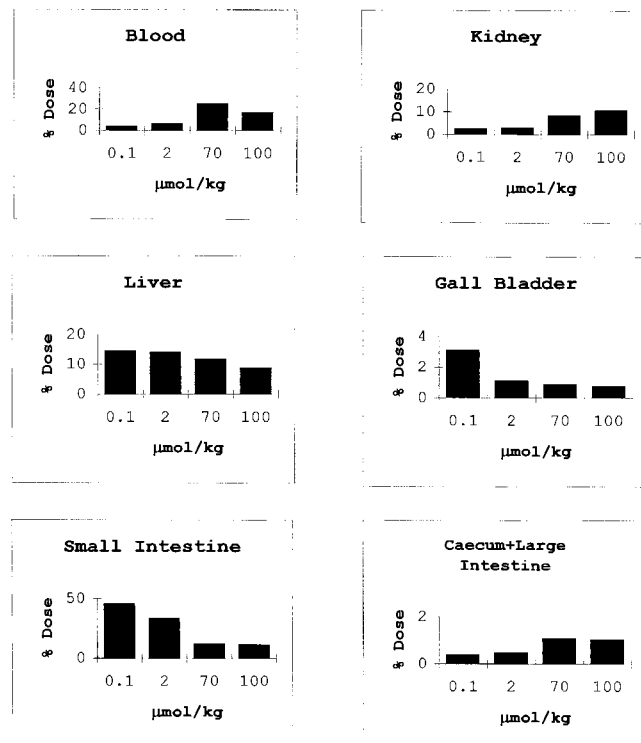

Fig. 4 Effect of the dose given on the biodistribution of [GdL^{1a}]$^-$ in mice, 5 min post administration

As the dose of [GdL^{1a}]$^-$ is increased (Fig. 4) saturation of the transporter sites in the liver cells may be occurring. This would have the effect of slowing down the rate of clearance of the
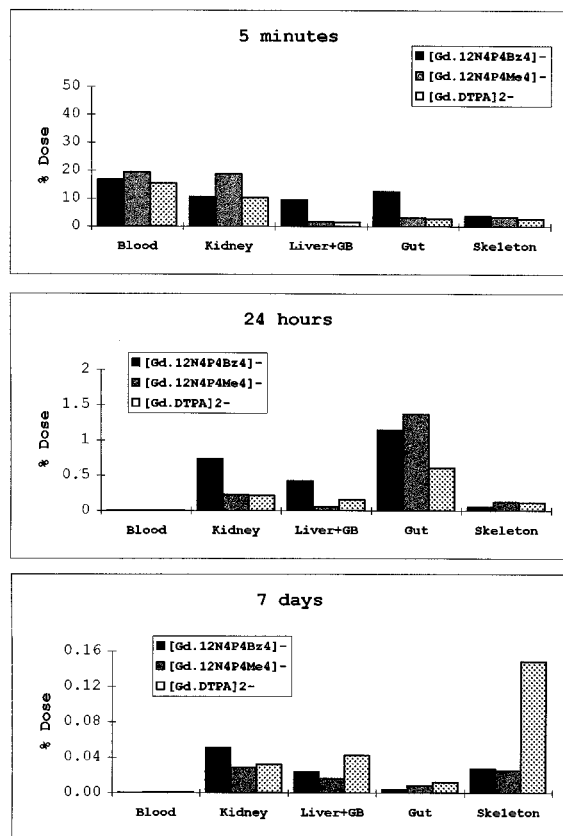
Comparative biodistribution 5 minutes, 24 hours, 7 days charts

Fig. 5 Comparative biodistribution data for [GdL^{1a}]$^-$ (black) compared to [GdL^{1b}]$^-$ (grey) and [Gd(dtpa)]$^{2-}$ (dotted) at a dose of 0.1 mmol kg^{-1}. GB = Gall bladder

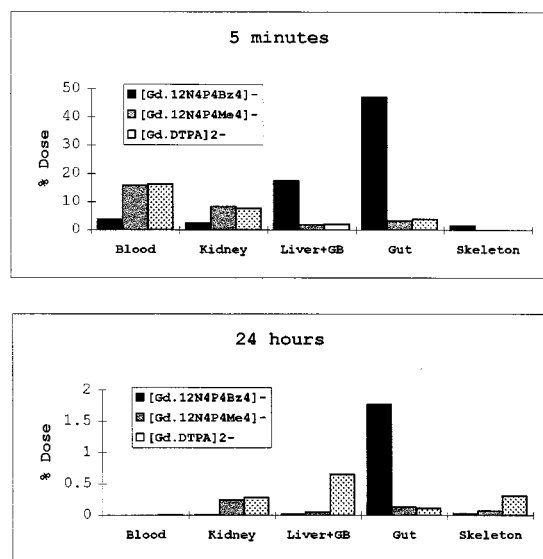**Fig. 6** Comparative biodistribution data at a dose of 0.1 μmol kg^{-1} for [GdL^{1a}]$^-$ (black) and the related hydrophilic complexes [GdL^{1b}]$^-$ (grey) and [Gd(dtpa)]$^{2-}$ (dotted)

complex *via* the hepatobiliary route. A consequence of this is that the % dose cleared by the renal route increases due to the higher circulating levels of complex in the blood. The anion bromosulfophthalein is known to block the receptors in the liver cells which are responsible for the transport of anionic lipophilic complexes.[20] If [GdL^{1a}]$^-$ is also handled by the organic anion transporter, then co-administration of sodium bromosulfophthalein should slow down the rate of passage of the complex through the biliary route. When 100 μg g^{-1} of bromosulfophthalein were administered to mice 2 min prior to injection of 0.1 mmol kg^{-1} of [GdL^{1a}]$^-$ a decrease was observed (Fig. 7) in the amount of the radiolabelled complex in

Table 2 Biodistribution data for C$_3$H mice bearing a subcutaneous RIF fibrosarcoma xenograft after administration of [GdL^{1a}]$^-$ (0.1 mmol kg^{-1}) *

Tissue	% injected dose per g tissue		
	1 h	2 h	7 h
Blood	2.23 (1.15)	0.53 (0.22)	0.01 (0.005)
Kidney	17.3 (11.7)	5.61 (2.23)	7.42 (2.78)
Liver	13.1 (4.3)	3.11 (0.73)	0.90 (0.28)
Femur	0.55 (0.25)	0.15 (0.05)	0.04 (0.01)
Muscle	0.34 (0.13)	0.09 (0.04)	0.013 (0.007)
Tumour	0.79 (0.38)	0.36 (0.07)	0.20 (0.03)

* Gadolinium-153 (γ, $t_{\frac{1}{2}}$ = 241 d) was used as the tracer. Mean values for at least four animals are given with standard deviations in parentheses.

Table 3 Biodistribution data for male nude mice * bearing a human melanotic melanoma xenograft (HX 118) after administration of [GdL^{1a}]$^-$ (0.1 mmol kg^{-1})

Tissue	% injected dose per g tissue	
	1 h	4 h
Blood	1.83	0.05 (0.05)
Kidney	11.0	6.98 (5.4)
Liver	6.20	1.13 (0.72)
Femur	0.50	0.05 (0.03)
Muscle	0.37	0.02 (0.01)
Tumour	1.29	0.52 (0.21)

* Mean values for five animals are given, with standard deviations in parentheses. At 1 h, reported values are the means for only three animals.
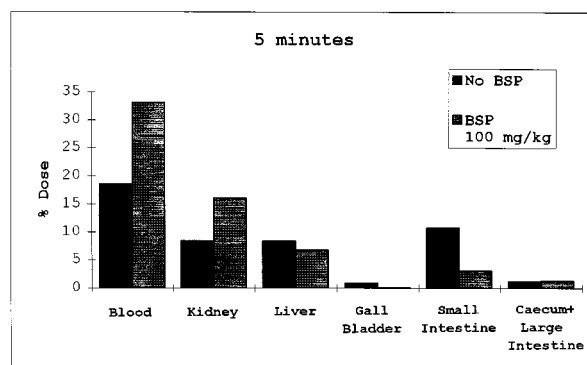

Fig. 7 Effect of co-administration of sodium bromosulfophthalein (BSP) on the biodistribution of [GdL^{1a}]$^-$, given at a dose of 0.1 mmol kg^{-1}

all tissues of the hepatobiliary route (liver, gall bladder, intestines). As a consequence, the amount of the complex in the blood is greater and there is an increase in the proportion of renal clearance.

This pattern of behaviour *in vivo* highlights the potential utility of [GdL^{1a}]$^-$ or its congeners in MRI studies. It may be administered at low doses for cholangiography, *e.g.* at 0.5 to 3 μmol dm^{-3} so that liver receptor sites are not saturated. Further work was then undertaken examining the behaviour of the complex in tumour-bearing animals. Using a dose of 0.1 mmol kg^{-1} (*i.e.* a typical clinical imaging dose), the biodistribution of ^{153}Gd-labelled complex was examined in mice bearing either a Rif fibrosarcoma or a xenograft of the human melanotic melanoma, HX 118. The former tumour is typically rather dense and poorly vascularised, whereas the latter is much less dense, tends to retain a good blood supply and commonly develops metastases in the liver and lung.

Data are presented in Tables 2 and 3, for the amounts of activity (expressed as the percentage of the injected dose per gram of tissue) in the given tissue type at periods of up to 7 h

Complex	$\tau(D_2O)$	$\tau(H_2O)$	q	$\varphi(D_2O)$	$\varphi(H_2O)$	φ_{fl}[b]
[TbL[1a]]$^-$	4.44	4.13	0.07	0.49	0.44	
[TbL[2]]$^-$	4.33	3.97	0.09	0.52	0.44	1
[TbL[3]]$^-$	4.42	4.08	0.08	0.46	0.40	0.91
[TbL[4]]$^-$	4.32	4.00	0.08	0.08	0.07	0.54

[a] Lifetimes are quoted in milliseconds, for $\lambda_{ex} = 277$ nm and $\lambda_{em} = 545$ nm. [b] Fluorescence quantum yields shown are relative to that of [TbL[2]]$^-$, which is arbitrarily set to 1.0.

post injection. In each case the rate of clearance of the complex from skeletal muscular tissue was similar to the rate of clearance from the blood, The rate of clearance of the complex from the tumour tissue was slower, so that the ratio of the amount of complex in the tumour to the amount in the surrounding muscle increased with time. In the fibrosarcoma-bearing animals, for example, this ratio increased from 2.3 (1 h) to 4 at 2 h and at 7 h the ratio was 15.3 : 1. A similar pattern was evident in the animals bearing the melanoma xenograft. In this case the tumour : muscle ratio increased from 3.5 (1 h) to 27.4 : 1 at 4 h. This differential rate of clearance of lipophilic anionic complexes from tumour tissue has been characterised previously in studies with manganese complexes of porphyrins.[22] It is consistent with the observation from *in vivo* MRI studies at similar doses that the site of subcutaneously implanted tumours in anaesthetised rats may be discerned increasingly easily at time points 5, 100 and 450 min post injection of 0.1 mmol kg^{-1} of [GdL[1]]$^-$.[23]

Luminescence studies

The luminescence behaviour of the europium and terbium complexes of L^2, L^3 and L^4 was investigated in water and D_2O, allowing comparison with the information obtained previously with complexes of L^{1a}. All the complexes showed the characteristic absorbance spectra of the methoxybenzyl chromophore ($\lambda_{max} = 274$ nm, $\varepsilon = 3800$ dm^3 mol^{-1} cm^{-1}). Using an excitation wavelength of 277 nm luminescence emission spectra for each of the six complexes were acquired. In each case the excitation spectra ($\lambda_{em} = 545$ nm for the terbium complexes and 619 nm for the europium complexes) closely resembled the corresponding absorption spectra. Such behaviour is consistent with efficient ligand-to-metal energy transfer, prior to metal-centred emission.[11]

The europium complexes gave very low overall quantum yields for emission, and the luminescence spectra obtained were rather weak, making precise lifetime determinations difficult. This behaviour may be ascribed to an efficient photoinduced electron-transfer process (PET) from the excited singlet state of the ligand to the metal. Such an electron-transfer process provides an efficient pathway for quenching of the aryl excited state, reducing the quantum yield for metal-based emission. Such behaviour is not at all unprecedented. Indeed similar observations having been made with the europium complex of a methoxybenzyl derivative of ethylenedinitrilotetraacetate (edta),[24] where the favourable free-energy change associated with the PET process was estimated to be of the order of -88 kJ mol^{-1}.

The terbium complexes exhibit much higher quantum yields and longer excited-state lifetimes, allowing more precise measurement of the luminescence decay. The results of these experiments, carried out at room temperature in water and D_2O, are summarised in Table 4. Comparison of the lifetimes obtained in water and D_2O allowed an assessment of the hydration state of these terbium complexes, estimated using the 'conventional' Horrocks analysis.[25,26] The values of q (the number of bound water molecules) using this analysis were of the order of 0.07 in all cases. These values are very similar to

those found with the terbium complex of L^{1a},[14] and clearly indicate that there is no metal-bound water molecule.

The *ortho*- and *meta*-substituted complexes show very high emissive quantum yields compared to those found for [TbL[1a]]$^-$, while that for the *para*-substituted complex is somewhat lower. The fluorescence quantum yields quoted in Table 4 are normalised relative to that found for the *ortho*-substituted complex; the pattern observed is similar. The fluorescence quantum yields are similar to those of the corresponding gadolinium complexes: the observed emission from Gd is extremely weak, indicating that energy transfer from the ligand singlet state to the metal may be neglected, consistent with energy transfer from the aryl triplet to the metal.[11]

The very high emissive quantum yields observed for [TbL[2]]$^-$ and [TbL[3]]$^-$ reflect in part the efficient shielding of the metal centre from vibrational quenching by the solvent and also indicate a limited role for other effective non-radiative decay pathways. These are the highest quantum yields reported for a 1:1 complex of terbium in aqueous solution. In addition to the shielding from energy-matched OH oscillators, the long lifetimes and high quantum yields may also be due to the absence of C=O oscillators in these complexes. Higher harmonics of C=O (ν_{CO} *ca.* 1610 cm^{-1}) may quench the emissive excited state, while P=O harmonics (ν_{PO} *ca.* 1150 cm^{-1}) are less likely to quench effectively.

Relaxivity measurements

The value of the measured relaxivity (the increment of the water proton nuclear magnetic longitudinal relaxation rate per unit concentration of the paramagnetic complex) and detailed analysis of the associated NMRD (magnetic field dependence of the relaxivity) profiles of gadolinium complexes allow a considerable amount of structural information to be obtained. In the case of [GdL[1a]]$^-$ the magnitude of the relaxivity and the nature and form of the NMRD profile have been shown to be consistent with the behaviour of a complex which does not possess any contribution from a bound water molecule.[14] Such behaviour accords with the conclusions of photophysical studies on the corresponding terbium and europium complexes, which exhibit small q values.[13] In addition, in the solid state, the crystal structures of the complexes of Y, Eu and Gd show no bound water (Figs. 1 and 2). In these cases, the relaxivity is simply attributed to the modulation of the nucleus–electron dipolar interaction by diffusion of the solvent molecules near the paramagnetic complex.[6] Quantitatively, its magnitude and magnetic field dependence are described by Freed's equation (1), in terms of the parameters a [the distance of minimum

$$R_{1p}^{OS} = (32\pi/405)\gamma_H^2 g^2 \mu_B^2 S(S+1)(N_a/1000)(M/aD) \times$$
$$[7J(\omega_S) + 3J(\omega_I)] \quad (1)$$

approach between the gadolinium(III) ion and the water protons], D (the relative diffusion coefficient for the solvent and the gadolinium complex) and the electronic relaxation time τ_s.

The NMRD profiles of the gadolinium complexes of the methoxy-substituted ligands L^2, L^3 and L^4 are very similar in form and nature to those reported previously for [GdL[1a]]$^-$ (Fig. 8).[14] The profiles for the three complexes are nearly superimposable in the high magnetic field region, where the relaxivity is controlled by a^2/D, whereas they are slightly different in the plateau region at lower fields where the contribution of τ_s becomes more important. This pattern of behaviour confirms the absence of proximate water molecules suggested by the luminescence measurements. Thus the NMRD profiles are fully consistent with gadolinium complexes of identical molecular size, co-ordination polyhedron and hydration sphere. The different substitution sites of the methoxy groups are distinguished by the slightly different τ_s values for the three complexes. Furthermore, the possibility of a tightly bound water
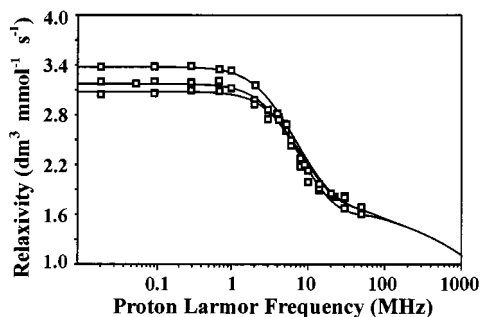
Fig. 8 Experimental NMRD profiles (298 K, pH 6.5) for (from the bottom to the top) $[GdL^2]^-$, $[GdL^3]^-$ and $[GdL^4]^-$. The solid lines through the data have been calculated with the 'best-fit' parameters to equation (1) for outer-sphere relaxation:[14] $a = 4.25$ Å, $D = 2.4$ cm^2 s^{-1}, $\tau_{SO} = 102$ ($[GdL^2]^-$), 115 ($[GdL^3]^-$), and 146 ps ($[GdL^4]^-$); $\tau_V = 16$ ($[GdL^2]^-$), 10 ($[GdL^3]^-$) and 13 ps ($[GdL^4]^-$) τ_V is the field-independent correlation time and τ_{SO} is the electronic relaxation time at zero field
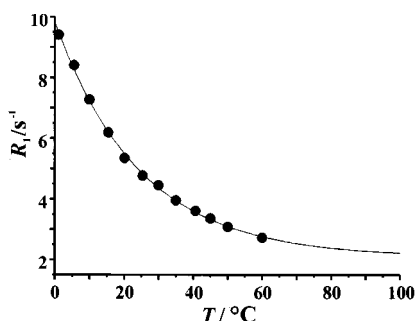

Fig. 9 Temperature dependence of the longitudinal relaxation rate for a 2.6 mmol dm^{-3} solution of $[GdL^3]^-$ at 20 MHz and pH 6.5
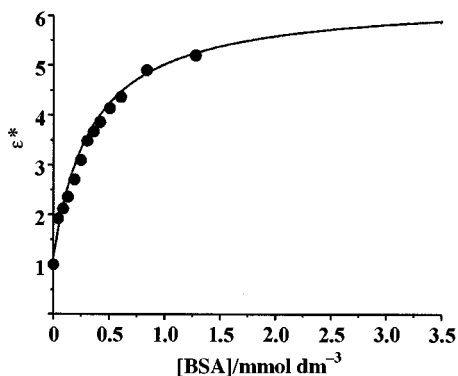

Fig. 10 Proton relaxation enhancement, ε^*, for $[GdL^3]^-$ (0.15 mmol dm^{-3}) at 20 MHz and 298 K, as a function of bovine serum albumin concentration. The term ε^* is defined as the ratio of the paramagnetic relaxation rates in the presence and absence of macromolecule. The solid line represents the best fit for a 1:1 complexation with $K_d = 1.1 \times 10^{-4}$ dm^3 mol^{-1}, as defined in ref. 14

molecule may effectively be ruled out from consideration of the temperature dependence of the relaxivities (Fig. 9). The temperature dependence of the measured NMRD profiles corresponds to that expected for purely 'outer-sphere' complexes that is simply described (at this magnetic field strength) by the monoexponential decrease of the diffusion coefficient D with temperature. In each case then the presence of the aryl methoxy group has not acted to increase the number of proximate water molecules, and the relaxivity behaviour remains that of purely 'outer-sphere' complexes.[6]

We had found previously that $[GdL^{1a}]^-$ forms a relatively strong complex with bovine serum albumin ($K_d = 2.8 \times 10^{-4}$ dm^3 mol^{-1}) leading to a marked relaxivity enhancement.[14] An analogous experiment with $[GdL^3]^-$ indicated that with this methoxy-substituted complex there was both a stronger interaction with the protein ($K_d = 1.1 \times 10^{-4}$ dm^3 mol^{-1}) and a significantly higher (*ca.* 20%) enhancement of the relaxivity (Fig.

10). Since a change of the co-ordination number of the metal ion upon interaction of the complex with albumin can be excluded, it is possible that this relaxivity increase may be attributed to the ability of the methoxy groups to promote the formation of a network of hydrogen-bonded water molecules in the second co-ordination sphere of the gadolinium(III) ion, near to the surface of the protein. This effect is not detected in aqueous solution because the mean residence lifetime of the hydrogen-bonded water molecules approaches the solvent translational diffusion correlation time. On the other hand, the high structural organisation and the consequent reduced mobility of the water molecules in the hydration sphere of the protein allows the observation of the second-sphere interactions which lead to an increase in the overall relaxivity.

^{31}P NMR Analysis of $[LnL^{1a}]^-$ complexes

Another possible means of probing the changes in structure of the lanthanide complexes across the series involves a comparison of the ^{31}P chemical shifts of the paramagnetic complexes with those of a diamagnetic analogue *e.g.* $[YL^{1a}]^-$. In general, the interaction of a lanthanide cation with an NMR-active nucleus in the ligand may be quantified in terms of two components.[27,28] The first involves a dipolar (or pseudo-contact) component arising from an electrostatic interaction between the metal ion and a Lewis base. The second is a contact contribution arising from the covalent character of local bonding interactions, where there is some transfer of unpaired electron-spin density to the ligand molecule. The latter effect tends to be significant only for nuclei proximate to the metal centre.

The observed shifts are additive, equation (2) where δ_{dia} is the

$$\delta_{obs} = \delta_{dia} + \delta_{dip} + \delta_{con} \qquad (2)$$

shift arising from an analogous diamagnetic ion (La^{3+}, Lu^{3+} or Y^{3+}), δ_{dip} is the pseudo-contact term and δ_{con} is the contact term. After correcting for the diamagnetic shift, the observed paramagnetic shift (LIS$_{obs}$) is given by the sum of the pseudo-contact and contact contributions, *i.e.* as in equation (3). It

$$LIS_{obs} = LIS_{pc} + LIS_c \qquad (3)$$

has been shown[29] that when a magnetic field, B, is applied to the system at a given temperature T, then the thermal average spin moment, $\langle S \rangle_{av}$, for all the J levels is given by equation (4)

$$\langle S \rangle_{av} = (\beta B/3kT)g_J(g_J - 1)J(J + 1) \qquad (4)$$

where $g_J = 1 + \{[J(J + 1) - L(L + 1) + S(S + 1)]/2J(J + 1)\}$. For a nucleus acted on by a lanthanide the change in effective magnetic field, ΔB, due to the contact interaction with unpaired f electrons is related by $\delta_{con} \propto \langle S \rangle_a$ thus $\delta_{con} \propto (g_J - 1)$. For the pseudo-contact term Bleaney *et al.*[30] carried out a theoretical treatment for a bound ligand with polar coordinates (r, θ), from which equation (5) may be derived, where

$$\delta_{dip} = C_J(\beta^2/60k^2T^2)\{(3\cos^2\theta - 1)/r^3\}P' \qquad (5)$$

$C_J = g^2J(J + 1)(2J - 1)(2J + 3)\langle J|\alpha|J\rangle$, $\langle J|\alpha|J\rangle$ is a numerical coefficient derived from matrix elements of J, and P' is a crystal-field coefficient which should remain constant for a given series of isostructural complexes. The signs and relative magnitudes of the values are thus dependent on C_J.

Substituting the terms back into equation (2) gives (6) in

$$LIS_{obs} = GC_J + F\langle S \rangle_{av} \qquad (6)$$

which G is the geometrical term in equation (3) and the term F contains the hyperfine coupling constant. Equation (6) may be rearranged to (7) and (8). For isostructural complexes a plot of
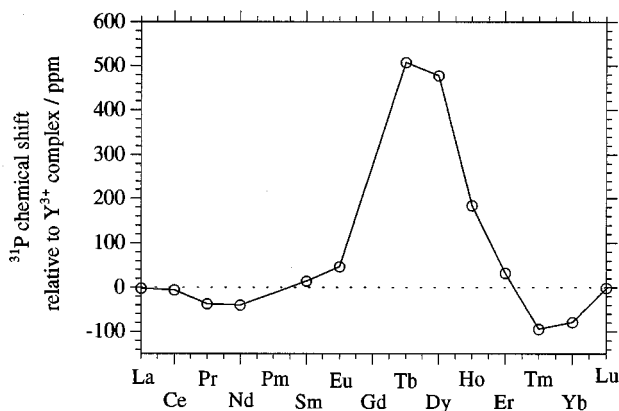
Fig. 11 Variation of the ^{31}P NMR shift for the lanthanide complexes of L^{1a} (pD 6.5, 293 K), relative to the diamagnetic yttrium complex
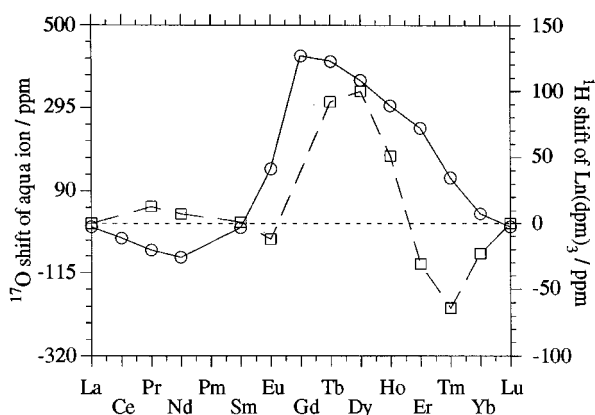

Fig. 12 Paramagnetic ^{17}O NMR shifts for the lanthanide aqua ions and ^{1}H NMR shifts for the complexes [Ln(dpm)₃] (Hdpm = dipivaloylmethane)
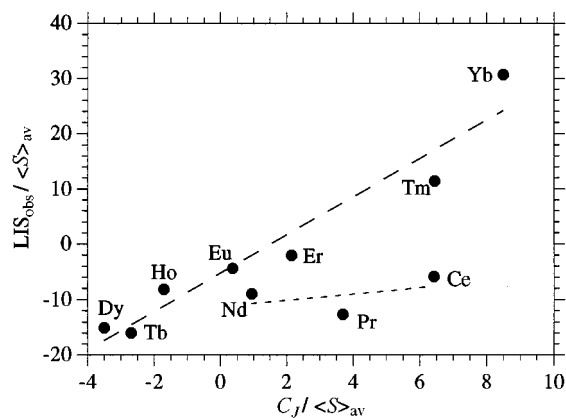

Fig. 13 Analysis of the ^{31}P NMR shifts for [LnL^{1a}]⁻, plotted according to equation (7)

$$\text{LIS}_{\text{obs}}/\langle S \rangle_{\text{av}} = G(C_J/\langle S \rangle_{\text{av}}) + F \qquad (7)$$

$$\text{LIS}_{\text{obs}}/C_J = G + F(\langle S \rangle_{\text{av}}/C_J) \qquad (8)$$

the observed shifts according to equation (7) or (8) should be a straight line.[31]

In the case of the lanthanide complexes [LnL^{1a}]⁻ the variation in δ_P with lanthanide relative to that of the yttrium complex (δ 39.4) has been measured (Fig. 11). This correlation may be compared to that obtained with the oxygen-17 *contact* paramagnetic shifts of the aqua ions and the ^{1}H shifts for the series [Ln(dpm)₃][17] where only the *pseudo-contact* contribution is relevant (Fig. 12). It may be seen that the pattern of behaviour resembles that of the oxygen-17 shifts more closely,
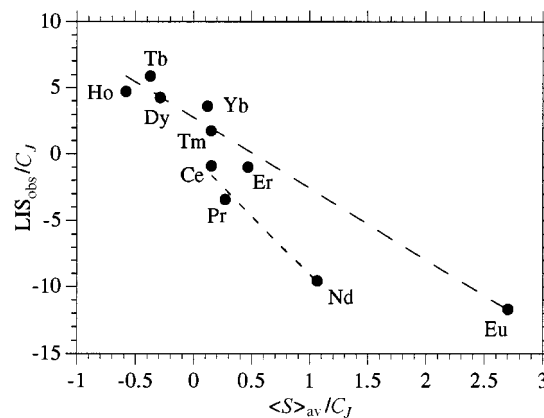

Fig. 14 Analysis of the ^{31}P NMR shifts for [LnL^{1a}]⁻, plotted according to equation (8)

suggesting a substantial contribution from the contact term. This is perhaps not surprising given the proximity of the phosphorus atoms in the complex to the bound lanthanide ion (*ca.* 3.35 Å), and the relatively high degree of spatial penetration by the phosphorus orbitals.

The plots according to equations (7) and (8) are shown in Figs. 13 and 14 respectively. This analysis suggests that the lanthanides fall into two groups, with the earlier larger lanthanide complexes (*i.e.* of Ce^{3+}, Pr^{3+} and Nd^{3+}) behaving similarly, associated perhaps with a different structure to those of the later lanthanides (Sm to Yb), which diverge less from a straight line. It has been suggested that in the analysis according to equation (8) such an apparent discontinuity may simply be a consequence of the change in ionic radius across the series, due to the variation in the polar coordinates of the ion without any change in overall structure.[32] However, there is a clear discontinuity here, in both Figs. 13 and 14. When these results are taken in conjunction with the established structure of the early and middle [LnL^{1a}]⁻ complexes, the analysis may be linked to the occurrence of two closely related types of structure, with only the larger early lanthanide ions (La to Pr/Nd) able to accommodate a bound water molecule in their co-ordination environment.

Conclusion

For L^{1a} there is a variation in structure of the lanthanide complexes across the series, associated with the decrease in ionic radius from La to Yb. The measurements outlined above have demonstrated that the earlier lanthanides and La tend to be nine-co-ordinate while the middle and later lanthanides are eight-co-ordinate and lack a bound water molecule. All of the lanthanide complexes of L^{1a} take up a twisted square-antiprismatic structure. The exclusion of a water molecule from the metal co-ordination site reduces the quenching of photo-excited states, prolonging the excited-state lifetime and possibly allowing the development of solubilised analogues of such ligands for time-resolved luminescence microscopy. Although the lack of an inner-sphere water molecule limits the overall relaxivity of the gadolinium complexes, their selective biliary clearance at low concentration of complex, their slower rate of clearance from tumour tissue combined with the substantial proton-relaxation enhancement effect observed in the presence of proteins such as albumin render them attractive complexes for MRI study.

Experimental

Commercial solvents were dried with the appropriate drying agent according to standard procedures. Water was purified by the Purite system. Proton and ^{13}C NMR spectra were recorded on Bruker AC-250 (250.1 and 62.9 MHz respectively) or Varian

Table 5 Crystal data for $[LnL^{1a}]^-$ and $[LnL^{1a}(H_2O)]^-$ complexes

	Y	La	Eu	Gd	Yb
T/K	295	150	150	155	150
Space group	$Pbcn$	$Pbcn$	$Pbcn$	$Pbcn$	$C2/c$
Symmetry	Orthorhombic	Orthorhombic	Orthorhombic	Orthorhombic	Monoclinic
a/Å	22.332(5)	22.744(1)	22.842(2)	22.949(4)	32.135(15)
b/Å	23.052(9)	23.124(1)	22.620(2)	22.718(4)	31.447(8)
c/Å	21.301(8)	21.198(1)	21.178(2)	21.128(4)	21.451(7)
β/°					93.98(3)
U/Å^3	10 965(7)	11 149(1)	10 942(2)	11 015(3)	21 624(13)
Z	8	8	8	8	16

VXR-400 spectrometers, ^{31}P NMR spectra on a Bruker AC-250 spectrometer operating at 101.1 MHz. Proton and carbon shifts are given to higher frequency of $SiMe_4$, while phosphorus shifts are referenced to an external sample of 85% aqueous phosphoric acid. Proton spectra of the terbium complexes were obtained on a Bruker AC-250 spectrometer operating with a sweep width of 500 ppm. Mass spectra were recorded on a VG 7070E and on a VG Platform II for electrospray mass spectrometry, high-resolution spectra at the Swansea EPSRC centre. Visible absorption spectra were acquired using a Uvikon 930 spectrophotometer. The HPLC analysis and separations were carried out on a Varian 5560 instrument fitted with a diode-array detector.

Variable-temperature proton–solvent longitudinal relaxation times were measured at 20 MHz on a Spinmaster spectrometer [Stelar, Mede(PV), Italy] by means of the inversion-recovery technique (16 experiments, four scans). The reproducibility in T_1 measurements was within less than 1%. The temperature was controlled by a Jael airflow heater equipped with a copper constantan thermocouple: the actual temperature in the probehead was measured with a Fluke 52 k/j digital thermometer with an uncertainty of 0.5 K.

The $1/T_1$ NMRD profiles of water protons were measured over a continuum of magnetic fields from 0.000 24 to 1.2 T corresponding to 0.01 to 50 MHz proton Larmor frequency on the Koenig-Brown field-cycling relaxometer installed at the University of Florence, Italy. The temperature inside the probe was controlled by circulation of perfluoroalkanes. Data at higher frequencies were also obtained from JEOL EX-90 and EX-400 spectrometers.

Crystallography

Single-crystal X-ray diffraction experiments were carried out at T 150 K, for the $[GdL^{1a}]^-$ complex on a Rigaku AFC6S four-circle diffractometer (ω-scan mode), for other complexes on a Siemens SMART three-circle diffractometer equipped with a CCD area detector (scanning a full hemisphere of reciprocal space by ω in 0.3° frames). Graphite-monochromated Mo-Kα radiation ($\bar{\lambda} = 0.710\ 73$ Å) and a Cryostream open-flow N_2 gas cryostat were used. The structures were solved by Patterson and Fourier methods and refined by full-matrix least squares against F^2 for all data using SHELXTL software.[33a]

Colourless orthogonal crystals of the complexes of La, Eu and Gd studied proved isomorphous (see Table 5) with the yttrium complex reported earlier, crystallising in the orthorhombic space group $Pbcn$ (no. 60), while the C-centred monoclinic lattice of the ytterbium complex can be interpreted as a distortion of the above-mentioned ones, its Niggli cell (in the corresponding setting) being $a = b = 22.539(8)$, $c = 21.490(7)$ Å, $\alpha = \beta = 87.15(3)$, $\gamma = 88.84(3)°$.

The crystals of all complexes were stable only in the presence of solvent or its vapour and quickly decomposed on drying. The structural study was much hindered by the quality of crystals, which exhibited weak high-angle diffraction and were extremely prone to twinning. The matters were further compli-

cated by the peculiar crystal packing. The structures contain ordered $[LnL^{1a}]^-$ anions (one per asymmetric unit, *i.e.* $Z = 8$), but wide (*ca.* 7.5 Å in diameter) channels between them, parallel to the crystallographic axis z, are occupied by numerous molecules of the solvent of crystallisation, most of them disordered (for $[YL^{1a}]^-$, 14 independent positions of water molecules were located). The way in which the crystals were obtained makes possible the presence, besides water, of alcohol of crystallisation as well. Another uncertainty is the nature of the counter ion, which may be a hydrated proton (as for $[YL^{1a}]^-$), or an alkali-metal cation (present in the course of the syntheses). It must be emphasised that the size of the cavity suffices to accommodate a cation of substantial size, *e.g.* hexaaquametal, without affecting the anion packing seriously.

For the $[EuL^{1a}]^-$ complex, 48 208 data with $2\theta \leqslant 52°$ were collected, of which 9766 were unique ($R_{int} = 0.166$); 7102 data with $I > 2\sigma(I)$ were regarded as observed. Slight (*ca.* 2%) decay was observed in the course of the data collection (13 h). A semiempirical absorption correction was applied, based on Laue equivalents and repeated measurements (at different azimuthal angles) of all strong reflections (transmission factors $T_{min} = 0.437$, $T_{max} = 0.820$). The Eu atom was located by the Patterson method, other atoms of the anion by a succession of Fourier syntheses. Within the cavity 20 symmetrically independent atomic positions were revealed. The strongest peak of electron density was interpreted as a Na^+ cation with a 50% occupancy. This cation is disordered over two positions, 0.79 Å apart, related *via* the crystallographic axis 2 $[\frac{1}{2}\ y\ \frac{3}{4}]$. Its environment (apart from spurious contacts due to disorder) consists of five aqua-ligands at distances of 2.31 to 2.66 Å. Another 19 peaks were treated as oxygen atoms; seven of them could be interpreted as water molecules in fully occupied positions (held by hydrogen bonds to the anion), two symmetrically disordered (50%) in the Na^+ environment. Elsewhere the electron-density map suggested the presence of disordered methanol and/or water molecules, in some cases probably sharing the same positions. Finally it was most effectively approximated by 10 oxygen atoms with occupancies of 2/3 each, linked pairwise to other such 'atoms' or their own symmetrical equivalents at distances of 0.9 to 1.65 Å.

Ordered non-H atoms were refined with anisotropic displacement parameters, closely positioned disordered atoms in isotropic approximation, making a total of 695 refined variables, converging at $R = 0.106$, $wR = 0.283$ (here and below R refers to $|F|$ for observed data, wR to F^2 for all data), goodness of fit $S = 2.10$. All H atoms in the anion were treated as 'riding' in calculated positions, solvent H atoms were neglected. The only conspicuous feature in the residual difference electron-density distribution are four peaks of 2.2–2.3 e Å^{-3} at *ca.* 1 Å from the Eu atom, and some diffuse electron density ($\leqslant 0.9$ e Å^{-3}) in the channel.

For the $[LaL^{1a}(H_2O)]^-$ complex it was not possible to obtain single crystals; from a deconvoluted twin, 27 104 reflections with $2\theta \leqslant 38°$ were used (4429 unique, $R_{int} = 0.104$, 3720 observed), the high-angle data being of insufficient quality. All atoms of the anion were found by Patterson and Fourier techniques. In

the cavity, 13 significant electron-density peaks were revealed. These were interpreted as molecules of crystallisation water (some of them disordered between two positions in close proximity) and refined as oxygen atoms (three as fully occupied positions and 10 with 50% occupancies). Phenyl rings were refined as rigid groups; La, P and anion O atoms were refined with anisotropic displacement parameters, other non-H atoms in isotropic approximation (total of 308 refined variables). The H atoms of the L[1a] ligand were treated as 'riding'; water H atoms were neglected. The refinement converged at $R = 0.199$, $wR = 0.48$, $S = 3.31$, residual $\Delta\rho_{max} = 1.38$, $\Delta\rho_{min} = -1.06$ e Å^{-3}.

For the gadolinium complex the lattice parameters have been determined and a full diffraction set of 7207 unique data with $2\theta \leqslant 45°$ was collected, but the reflections were exceedingly weak [average $I/\sigma(I) < 4$]. The systematic absences and the heavy-atom positions (from the Patterson map) show clearly that the crystal is isostructural with those of the complexes of Y, La and Eu. However, because of insufficient resolution, neither full structure determination nor refinement of atomic coordinates from isostructural complexes gave satisfactory results.

For the ytterbium complex, 87 025 data with $2\theta \leqslant 55°$ were collected (24 920 unique, 18 184 observed, $R_{int} = 0.082$ after a SADABS absorption correction,[33b] $T_{min} = 0.41$, $T_{max} = 0.70$). The structure was solved by Patterson and Fourier methods, revealing the entire [YbL[1a]]$^-$ anion, a [K(H$_2$O)$_6$]$^+$ anion and 16 water molecules of crystallisation (some of them disordered) in the channel. However, the refinement (Yb and P atoms anisotropic, other non-H atoms isotropic, phenyl rings as rigid groups, H atoms of L[1a] riding, total of 497 variables) gave irreducible $R = 0.25$, $wR = 0.48$, $S = 5.22$, the high residual features of electron density ($\Delta\rho_{max} = 9.2$, $\Delta\rho_{min} = -6.3$ e Å^{-3}) being in the close vicinity of the Yb atom. The peculiar form of the diffraction peaks (sharp in two dimensions and showing 'streaks' in the l direction) suggest exceedingly anisotropic mosaicity, disorder or incommensurate structure associated with the channels (see above).

CCDC reference number 186/659.

Luminescence measurements

Luminescence spectra were recorded using a Perkin-Elmer LS50B spectrofluorimeter operating in time-resolved mode and equipped with a Hamamatsu R928 photomultiplier tube. Phosphorescence excitation spectra were obtained by monitoring emission at 619 nm for europium(III) and 545 nm for terbium(III). Quoted lifetimes, τ, are the average values obtained from at least five measurements on each complex, made by monitoring the emission intensity after 20 different delay times spanning at least two lifetimes. Slit widths of 15 nm and a gate time of 0.1 ms were used and the phosphorescence decay curves fitted by an equation of the form (9). In all cases, high

$$I = I_0 \exp(-t/\tau) \qquad (9)$$

correlation coefficients were observed, and the lifetimes were found to be independent of concentration.

Luminescence quantum yields were obtained by the method of Haas and Stein,[34] using the quantum yield of [TbL[1a]]$^-$ as a standard ($\varphi = 0.49$ in D$_2$O).[13,15] The observed phosphorescence (P) for a cycle time of 20 ms was related to the total phosphorescence emission (P_T) by expression (10) where t_d is the delay time and t_g the gate time in ms.

$$P_T/P = \frac{1 - \exp(-20/\tau)}{\exp(-t_d/\tau) - \exp[-(t_d + t_g)/\tau]} \qquad (10)$$

Biodistribution studies

Batches of [^{153}GdL[1a]]$^-$ were prepared as described in ref. 12, and where appropriate were mixed with [^{157}GdL[1a]]$^-$ to the desired total concentration in phosphate-buffered saline (pH 7.4). The mixture was vortexed and filtered by centrifugation through a 0.22 μm Millipore Ultrafree CM filter. Mice were injected through the tail vein and the procedures used to establish the tissue biodistribution at the given times post-injection followed the methods previously described.[12,35]

Mice (C3H) bearing a subcutaneous implant in the mid-dorsal region of the murine fibrosarcoma Rif were injected intravenously with up to 200 μdm^{-3} of the solution of the complex. Typically the tumour weights were in the region 95 to 300 mg (cf. body weight of 25 to 30 g). Experiments involving nude male mice bearing the HX 118 melanotic melanoma xenograft followed the methods and practices set out previously.[35,36]

Syntheses

Compound L[1a] and its complexes were prepared as previously reported.[14]

Diethoxy(2-methoxybenzyl)phosphine 1a. To magnesium turnings (7.5 g) (previously dried at 60 °C under high vacuum) under argon were added sodium-dried diethyl ether (100 cm^3) and a few grains of iodine. The solution was stirred at room temperature until the purple colour of the iodine disappeared and the mixture was heated to reflux. To the vigorously stirred solution was slowly added (over 2 h) o-methoxybenzyl chloride (4.75 g, 0.030 mol) in ether (20 cm^3). The solution was stirred for 30 min, filtered under argon and completion of Grignard formation confirmed by addition of D$_2$O to a small sample, followed by ^{1}H NMR analysis of the CH$_2$D resonance. To the solution of the Grignard reagent cooled to -40 °C was slowly added over 1 h diethyl chlorophosphite (4.27 g, 0.27 mol, 0.9 equivalent). The solution was allowed to warm to room temperature overnight, filtered under argon, and complete conversion into the phosphine (δ_P +176) confirmed by ^{31}P NMR analysis. It may be noted that removal of the solvent under vacuum led to decomposition of the phosphine which necessitated its use in subsequent steps as a standardised ether solution.

Diethoxy(3-methoxybenzyl)phosphine 1b. 3-Methoxybenzyl chloride (6.42 g, 41 mmol) was added to a stirred suspension of magnesium turnings (2 g, excess) in tetrahydrofuran (40 cm^3), and a crystal of iodine was added. After an incubation period of 10 min a vigorous reaction commenced. The reaction mixture was stirred for 1 h, and the solution boiled under its own exotherm. The quality of the Grignard reagent was assessed by quenching a sample in D$_2$O. The NMR intensities revealed almost quantitative conversion. (The reaction has also been realised in dry ether.) An ether solution of the Grignard reagent ($\approx$24 mmol) was filtered via a steel cannula, to remove unchanged magnesium. Diethyl chlorophosphite (3.6 cm^3, 3.88 g, 24 mmol) was added at -20 °C. The product was not isolated in a pure form as the compound exhibits a propensity to decompose when distilled. δ_H(CDCl$_3$) 1.23 (6 H, t, CH$_3$), 2.95 (2 H, d, $J = 3.9$, CH$_2$P), 3.81 (3 H, s, OMe), 3.89 (4 H, dq, $J = 14$ Hz, OCH$_2$), 6.8 (3 H, m, aryl) and 7.2 (1 H, t, aryl). δ_C(CDCl$_3$) 16.9 (CH$_3$), 42.7 (CH$_2$P, d, $J = 21$), 54.8 (OCH$_3$), 62.9 (CH$_2$O, d, $J = 14$ Hz), 111.2, 112.4, 114.8, 121.8, 130.0 and 159.1. δ_P(CDCl$_3$) 176.8 (s). $\tilde{\nu}_{max}$(film) 2974, 1600, 1490, 1198 and 1163 cm^{-1}. Desorption chemical ionisation (DCI) mass spectrum: m/z 243 (M^+ + 1).

Diethoxy(4-methoxybenzyl)phosphine 1c. This compound was prepared as described above, and again the product was used as a ^{31}P NMR standardised solution without being purified by distillation. δ_P(CDCl$_3$): 177.1 (s). DCI mass spectrum: m/z 243 (M^+ + 1).

Tetraethyl 1,4,7,10-tetraazacyclododecane-1,4,7,10-tetryl-tetramethylenetetra(2-methoxybenzylphosphinate) 2a. To 1,4,7, 10-tetraazacyclododecane (282 mg, 1.64 mmol) in sodium-

dried thf (80 cm³) at 110 °C under argon were added diethoxy-(2-methoxybenzyl)phosphine **1a** (2.38 g, 9.83 mmol) in ether (25 cm³), at which point the solution turned slightly cloudy, followed immediately by paraformaldehyde (451 mg, 15.0 mmol). The solution was boiled under reflux overnight with removal of water using a Soxhlet apparatus containing 4 Å molecular sieves. A clear yellow solution resulted which, on removal of the solvent under reduced pressure, yielded a crude yellow viscous oil. Purification by gradient alumina column chromatography (0 to 3% methanol in dichloromethane) yielded the product (762 mg, 44%) as a colourless oil. δ_P(CDCl$_3$) 50.0 (s). δ_H(CDCl$_3$) 1.14 (12 H, t, CH$_2$CH_3), 2.8–2.9 (24 H, br, NCH$_2$), 3.27 (8 H, d, J = 15 Hz, PCH_2C$_6$H$_4$), 3.80 (12 H, s, CH$_3$), 4.00 (8 H, m, OCH$_2$), 6.88 (8 H, m, CH_2CHCOMe) and 7.23 (8 H, m, CHCOMe, CHCCH$_2$Cl). δ_C(CDCl$_3$) 16.2 (4 C, CH$_3$), 29.0 (4 C, d, ^1J = 81 Hz, PCH_2C$_6$H$_4$), 53.8 (4 C, d, ^1J = 90 Hz, NCH$_2$P), 53.5 [8 C, (CH$_2$)$_2$N], 55.0 (4 C, OCH$_3$), 60.2 (4 C, OCH$_2$), 110.2, 120.3, 127.6, 131.0 (16 C, CH aromatic), 127.8 (4 C, CCH$_2$P) and 156.7 (4 C, COMe). DCI mass spectrum: m/z 1076.45 (M^+) and 1077.56 (M + H$^+$) (C$_{52}$H$_{80}$N$_4$O$_{12}$P$_4$ requires 1076.48).

Tetraethyl 1,4,7,10-tetraazacyclododecane-1,4,7,10-tetryltetramethylenetetra(3-methoxybenzylphosphinate) 2b. To a stirred solution of 1,4,7,10-tetraazacyclododecane (475 mg, 2.76 mmol) and paraformaldehyde (414 mg, 13.8 mmol), boiling under reflux over 4 Å molecular sieves in thf and under an argon atmosphere, was added diethoxy(4-methoxybenzyl)-phosphine (2.78 g, 11.5 mmol). A very pale orange precipitate was formed almost immediately, and the remaining solution became pale orange and slightly turbid, before heating was stopped after 6 h. Column chromatography (using the conditions defined above for **2a**) of the derived residue afforded the tetraester as a pale yellow glass, 528 mg (18%). HPLC: Spherisorb 5ODS2 (1.4 cm³ min⁻¹); elution A = MeCN–CF$_3$CO$_2$H; B = water–CF$_3$CO$_2$H from 5% A, 95% B to 95% A, 5% B over 30 min; observed λ = 278 nm; t_R = 24.8 min (broad). δ_H(CDCl$_3$) 1.71 (12 H, t, CH$_3$), 2.80 (24 H, m, CH$_2$N), 3.20 (8 H, m, C$_6$H$_4$CH_2), 3.75 (12 H, s, OMe), 3.8–4.2 (8 H, m, OCH$_2$), 6.48 (12 H, m, aryl) and 7.17 (4 H, t, aryl). δ_C(CDCl$_3$) 16.5, 35.8 (CH$_2$P, d, ^1J = 81), 52.2 (NCH$_2$P, d, ^1J = 106 Hz), 53.5 (CH$_2$N), 55.1 (OCH$_3$), 60.8 (OCH$_2$), 112.1, 115.5, 122.2, 129.4 (aryl C), 132.9 (quaternary C) and 159.5 (COMe). δ_P(CDCl$_3$) 49.3. $\tilde{\nu}_{max}$(film): 2980, 2835, 1663, 1600, 1498, 1452, 1298, 1268, 1213 and 1151 cm⁻¹. Chemical ionisation (CI): m/z 1077 (M^+ + 1), 215 (100%). FAB mass spectrum (polyethylene glycol matrix): m/z 1077.480 (C$_{52}$H$_{81}$N$_4$O$_{12}$P$_4$ requires 1077.480).

Tetraethyl 1,4,7,10-tetraazacyclododecane-1,4,7,10-tetryltetramethylenetetra(4-methoxybenzylphosphinate) 2c. To a stirred solution of 1,4,7,10-tetraazacyclododecane (230 mg, 1.34 mmol) and paraformaldehyde (180 mg, 6.1 mmol) refluxing through a Soxhlet apparatus containing 4 Å molecular sieves in dry tetrahydrofuran (50 cm³) under an argon atmosphere was added a solution of diethoxy(4-methoxybenzyl)-phosphine (1.5 g, 6 mmol) in thf (25 cm³). Upon addition a vigorous exothermic reaction was observed and a deep yellow colour developed, after which the reaction was heated under reflux for 18 h. Solvent was removed under reduced pressure, and the residue purified by column chromatography on neutral alumina with gradient elution from 100% CH$_2$Cl$_2$ to 3% methanol in CH$_2$Cl$_2$. The ester (R_f = 0.6, 5% MeOH–95% CH$_2$Cl$_2$) was isolated as a viscous pale yellow oil, 340 mg (24%). δ_H(CDCl$_3$) 1.16–1.30 (12 H, m, CH$_3$), 2.64–3.22 (32 H, m, CH$_2$N and C$_6$H$_4$CH_2), 3.79 (12 H, s, OMe), 3.90–4.22 (8 H, m, OCH$_2$), 6.84–6.87 (8 H, m, aryl) and 7.21–7.26 (8 H, m, aryl). δ_C(CDCl$_3$) 17.2, 35.7 (CH$_2$P, d, ^1J = 82 Hz), 53–55 (m, ring CH$_2$N), 55.6, 61.1, 68.3, 114.4, 123.7, 129.4, 131.3 and 158.9. δ_P(CDCl$_3$) 49.9. DCI mass spectrum: m/z 1077.51 (M + H$^+$).

1,4,7,10-Tetraazacyclododecane-1,4,7,10-tetryltetramethylenetetra(2-methoxybenzylphosphinic acid) H$_4$L^2. The ester **2a** (283 mg, 0.26 mmol) was dissolved in methanol (1.5 cm³) and added to a solution of potassium hydroxide (590 mg) in water (17.5 cm³). The solution was heated at 70 °C for 24 h and the progress of the hydrolysis followed by ^{31}P NMR spectroscopy. Once reaction was judged to be complete, the pH was lowered to 6 with aqueous hydrochloric acid solution (6 mol dm⁻³) and following removal of the water by lyophilisation the product was purified by HPLC using an AX100 anion-exchange column (t = 0 min, 20% MeCN, 70% water, 10% 0.1 mol dm⁻³ NH$_4$O$_2$CMe, pH 5.5; t = 20 min, 20% MeCN, 0% water, 80% 0.1 mol dm⁻³ NH$_4$O$_2$CMe, pH 5.5) to yield a colourless solid (t_R = 12.1 min), 128 mg. δ_P(D$_2$O, pD 14) 37.2. δ_H(D$_2$O) 2.82, 2.90, 3.01 (32 H, NCH$_2$, PCH$_2$), 3.63 (12 H, s, OCH$_3$), 6.84 [8 H, m, (CH)$_2$CHCOMe] and 7.11 (8 H, m, CHCOMe, CHCCH$_2$P); δ_C(D$_2$O) 35.7 (4 C, d, ^1J = 89, PCH_2C$_6$H$_4$), 53.9 [8 C, m, (CH$_2$)$_2$N], 54.8 (8 C, d, ^1J = 84, NCH$_2$P), 58.3 (4 C, OCH$_3$), 114.1 (4 C, CHCHCOMe), 123.7 (4 C, d, J = 2.3, CHCHCH$_2$P), 124.8 (4 C, d, J = 8, CCH$_2$P), 131.0 (4 C, d, J = 3.0, CHCOMe), 134.2 (4 C, d, J = 5.0, CHCCH$_2$P) and 159.6 (4 C, d, J = 5.0 Hz, COMe). Positive-ion electrospray mass spectrum: m/z 987.55 (M + Na$^+$) and 965.59 (M + H$^+$).

1,4,7,10-Tetraazacyclododecane-1,4,7,10-tetryltetramethylenetetra(3-methoxybenzylphosphinic acid) H$_4$L^3. This compound was prepared as for L². A small amount of the *meta*-substituted ligand was purified by HPLC for characterisation purposes. HPLC: Synchropak AZ100 (5 cm³ min⁻¹); elution A = MeCN, B = water, C = NH$_4$O$_2$CMe, pH 5.6 from 20% A, 70% B, 10% C to 20% A, 0% B, 80% C in 20 min, t_R = 13.1 min. δ_H(D$_2$O) 2.8–3.2 [32 H, m (maxima at 2.82, 2.91, 3.09), CH$_2$N + C$_6$H$_4$CH$_2$], 3.65 (12 H, s, OMe), 6.76 (12 H, br s, aryl H) and 7.16 (4 H, t, aryl H). δ_C(D$_2$O, pD 5) 41.2 (C$_6$H$_4$CH_2P, d, ^1J = 87), 54.0 (CH$_2$N ring), 54.1 (NCH$_2$P, d, J = 93), 58.1 (OMe), 115.1 ($^4J_{CP}$ = 2.8), 118.2 ($^3J_{CP}$ = 5.4), 125.5 ($^3J_{CP}$ = 5.3), 132.8 ($^5J_{CP}$ = 2.6), 137.7 (^2J = 8.0) and 161.8 ($^4J_{CP}$ = 2.8 Hz). δ_P(D$_2$O, pD 3) 31.9 (br). Negative ion electrospray mass spectrum: m/z 1003.4 (100%, M + K$^+$).

1,4,7,10-Tetraazacyclododecane-1,4,7,10-tetryltetramethylenetetra(4-methoxybenzylphosphinic acid) H$_4$L^4. The ester **2c** (283 mg, 0.26 mmol) was dissolved in methanol (1.5 cm³) and added to an aqueous solution containing potassium hydroxide (590 mg) in water (17.5 cm³). The solution was heated at 70 °C for 24 h and the progress of the hydrolysis followed by ^{31}P NMR spectroscopy. Once complete, the pH was adjusted to 2 and the resulting white precipitate filtered off, dried and recrystallised from MeOH to yield the product as a white crystalline solid (120 mg, 48%), m.p. 146 °C (decomp.). δ_H(D$_2$O) 2.8–3.6 (32 H, m, CH$_2$N + C$_6$H$_4$CH$_2$), 3.82 (12 H, s, OMe), 6.84–6.90 (8 H, m, aryl H), 7.18–7.25 (8 H, m, aryl H). δ_C(D$_2$O, pD 2) 41.2 (d, ^1J = 87), 51–54 (m, CH$_2$N ring), 53.8 (NCH$_2$P, d, ^1J = 90 Hz), 60.8 (OMe), 114.5, 123.6, 132.3 and 159.0. δ_P(D$_2$O, pD 2) 22.1 and 36.0 at pD 8. Positive-ion electrospray mass spectrum: m/z 987.6 (100%, M + Na$^+$).

[LaL^{1a}]⁻. The compound H$_4$L^{1a} (210 mg, 0.256 mmol) was dissolved in water (25 cm³). To this was added lanthanum oxide (41.6 mg, 0.5 equivalent) and the mixture was stirred for 8 h at 80 °C. The pH was modified to 6–7 (addition of aqueous NaOH), and the reaction left to continue for 3 h. The reaction mixture was allowed to cool and a colourless solid was filtered off. The complex was recrystallised from warm water to give colourless crystals which became opaque on losing water of crystallisation *in vacuo* (201 mg, 77%). δ_H(D$_2$O, pD ≈6) 2.01 (4 H, d, J = 13, CH$_2$), 2.18 (8 H, d, J = 13 Hz, CH$_2$), 3.0–3.6 (20 H, br m, CH$_2$), 7.14 (4 H, br m, aryl H) and 7.22 (16 H, br m, aryl H). δ_C(pD 6) 41.4 (d, J_{CP} = 92, C$_6$H$_4$CH_2P), 54.6 (d, ring carbon *anti* to C–P bond, J_{CP} = 12 Hz), 56.7 (ring CH$_2$N), 58.5

(d, $J_{CP} = 98$, NCH$_2$P), 129.2, 131.5 (aryl), 132.8 (d, $^3J_{CP} = 5$, aryl) and 136.7 (d, $^2J_{CP} = 8$ Hz, quaternary aryl). δ_P(pD 6) 37.6 and 38.8 (ratio $\approx$8:1). $\tilde{\nu}_{max}$(KBr disc) 1654, 1601, 1495, 1453, 1233, 1167, 1124 and 1026 cm^{-1}. Negative-ion electrospray mass spectrum: m/z 979.24 (C$_{40}$H$_{52}$LaN$_4$O$_8$P$_4$ requires 979.18). M.p. >250 °C (decomp.) (Found: C, 41.1; H, 6.69; N, 4.48. C$_{40}$H$_{53}$LaN$_4$O$_8$P$_4$·10H$_2$O) requires C, 41.4; H, 6.33; N, 4.83%).

[PrL^{1a}]$^-$. The tetrabenzylphosphinic acid H$_4$L^{1a} (134 mg, 0.159 mmol) and praseodymium nitrate hexahydrate (69 mg, 0.159 mmol) were stirred for 18 h in water (10 cm^3, pH 5) at 80 °C. On cooling a colourless solid was filtered off (51 mg, 31%). δ_H(pD $\approx$6) −37.1 (4 H, axial ring CHN), −3.8 (4 H), −1.1 (4 H), 7.8 (4 H), 8.9 (4 H), 9.1 (8 H), 11.1 (8 H), 11.8 (4 H), 14.1 (4 H), 16.9 (4 H) and 32.6 (4 H). δ_C(pD 6) 14.0 (d, $J_{CP} = 100$), 36.0, 52.3, 53.2, 76.7 (d, $J_{CP} = 87$ Hz), 128.8, 130.7, 132.6 and 139.0. δ_P(pD 5.5) 34.2. $\tilde{\nu}_{max}$(film) 1656, 1552, 1500, 1456, 1158 and 1032 cm^{-1}. Negative-ion electrospray mass spectrum: m/z 980.21 (C$_{40}$H$_{52}$N$_4$O$_8$P$_4$Pr requires 981.18). M.p. >250 °C.

[YbL^{1a}]$^-$. The compound H$_4$L^{1a} (95 mg, 0.113 mmol) and ytterbium oxide (22.2 mg, 0.056 mmol) were stirred at 80 °C for 18 h. The pH of the solution was raised to 6, by addition of aqueous potassium hydroxide, and stirring continued for 4 h. The product, isolated by lyophilisation as a white solid, was soluble in weakly basic solution (pH > 7.5) and was recrystallised from such a solution (81 mg, 69%). δ_H(pD $\approx$10.5) −68.2, −35.4, −28.4, −9.4, −2.8, 2.7 (t), 7.4 (2 H, m), 14.9 (2 H, m), 18.6 (2 H, m), 19.7, 33.0 (2 H) and 104.0. δ_P(pD 10) −40.7. Negative-ion electrospray mass spectrum: m/z 1014.7 (C$_{40}$H$_{52}$N$_4$O$_8$P$_4$Yb requires 1014.2) (Found: C, 40.8; H, 6.09; N, 4.52. C$_{40}$H$_{53}$N$_4$O$_8$P$_4$Yb·8H$_2$O requires C, 41.1; H, 5.94; N, 4.79%).

General procedures for the complexes of Eu, Tb and Gd. To approximately 15 mg of ligand in water (2 cm^3) were added 1.1 equivalents of either europium, terbium or gadolinium acetate, and the pH adjusted to 6 (aqueous NaOH solution). The solutions immediately turned opaque, and were heated at 70 °C overnight to ensure complete complexation. The europium 2-methoxybenzyl complex and the 3-methoxybenzyl complexes were sufficiently soluble (4 mg cm^{-3}) to permit preparative anion-exchange HPLC purification, but the lack of solubility of the other complexes necessitated removal of the water under vacuum followed by an aqueous wash of the remaining insoluble solid complexes to remove any excess of metal acetate. All complexes gave molecular ions in electrospray mass spectroscopy, which were verified as the metal complexes by comparison with the theoretical mass isotope distributions.

[H$_3$O][EuL^2]: δ_P(D$_2$O, pD 5.5) 89.6 (s); δ_H(D$_2$O, pD 6) −13.5 (4 H, NCH'P), −7.9 (4 H, NCHP), −4.7 (4 H, H$_{ax'}$, CHN ring), −4.3 (4 H, H$_{eq'}$, CHN ring), −0.6 (4 H, aryl CHP), 1.3 (4 H, aryl CH'P), 2.4 (4 H, H$_{eq}$, CHN), 3.8 (12 H, OMe), 7.85 (4 H, p-H), 8.7 (4 H, m-H), 10.2 (8 H, m-H), 16.5 (4 H, o-H) and 29.5 (4 H, H$_{ax}$, CHHN ring) (Found: C, 39.5; H, 6.15; N, 4.30. C$_{44}$H$_{61}$EuN$_4$O$_{12}$P$_4$·5H$_2$O requires C, 39.9; H, 5.90; N, 4.65%).

[H$_3$O][TbL^2]: δ_P(D$_2$O, pD 5.5) 542 (s).

[H$_3$O][TbL^3]: purified by HPLC on Synchropak AX100 (1.4 cm^3 min^{-1}), elution A = MeCN, B = water, C = NH$_4$O$_2$CMe, pH 5.6 from 20% A, 70% B, 10% C to 20% A, 0% B, 80% C in 20 min, t_R = 9.7 min; δ_H(D$_2$O) −198 (vbr), −126 (br), −117 (br), −93, −73 (br), −57, −42 (12 H), 35 (vbr), 51 (br), 140 (vbr), 199 (vbr) and 290 (vbr); δ_P(D$_2$O) 441 (br); $\tilde{\nu}_{max}$(KBr) 3404, 1600, 1487, 1297, 1268, 1231, 1168 and 1119 cm^{-1}; UV (H$_2$O) λ_{max} = 273 and 278 nm (ε = 3.6 × 10^3 dm^3 mol^{-1} cm^{-1}); τ(H$_2$O) = 4.08, τ(D$_2$O) = 4.42 ms, q = 0.08; φ(H$_2$O) = 0.40, φ(D$_2$O) = 0.46; negative-ion electrospray mass spectrum: m/z 1119.3, 1120.3 and 1121.3 (C$_{44}$H$_{60}$N$_4$O$_{12}$P$_4$Tb requires 1119.24); m.p. >250 °C (decomp.).

[H$_3$O][EuL^3]: Synchropak AX100 (5 cm^3 min^{-1}), elution A = MeCN, B = water, C = NH$_4$O$_2$CMe, pH 5.6 from 20% A, 70% B, 10% C to 20% A, 0% B, 80% C in 20 min, t_R = 11.9 min; δ_H(pD 6) −18.0 (4 H, NCHP), −11.4 (4 H, NCH'P), −7.4 (4 H, H$_{ax'}$, CHN ring), −4.8 (4 H, H$_{eq'}$, CHN ring), −1.6 (4 H, H$_{eq}$, CHN ring), 0.4 [8 H, d (collapses to a singlet on {^{31}P}], 5.3 (12 H, OMe), 8.5 (4 H, p-H), 10.4 (4 H, m-H), 10.6 (4 H, o-H), 14.2, (4 H, o-H) and 34.3 (4 H, H$_{ax}$, CHN ring); δ_P(pD 6) 87.2; $\tilde{\nu}_{max}$(KBr) 3428, 3148, 3058, 1610, 1488, 1406, 1266, 1229, 1165, 1117 and 1030 cm^{-1}; UV (H$_2$O) λ_{max} = 273 and 278 nm (ε = 3.8 × 10^3 dm^3 mol^{-1} cm^{-1}); negative-ion electrospray mass spectrum: m/z 1111.3, 1113.2 and 1114.2 (most abundant ion C$_{44}$H$_{60}$EuN$_4$O$_{12}$P$_4$ requires 1113.24); m.p. >250 °C.

[H$_3$O][GdL^3]: HPLC, t_R = 13.3 min; NMR spectra could not be obtained due to line broadening by the paramagnetic broadening induced by the gadolinium ion; $\tilde{\nu}_{max}$(KBr) 3419, 1654, 1601, 1487, 1405, 1266, 1229, 1167, 1117 and 1027 cm^{-1}; UV (H$_2$O) λ_{max} = 273 and 278 nm; negative-ion electrospray mass spectrum: m/z 1115.3, 1116.3, 1117.3, 1118.39 (most abundant ion C$_{44}$H$_{60}$GdN$_4$O$_{12}$P$_4$ requires 1118.24), 1119.6, 1120.4 and 1121.4 (Found: C, 42.9; H, 5.96; N, 4.37. C$_{44}$H$_{61}$GdN$_4$O$_{12}$P$_4$·5H$_2$O requires C, 43.3; H, 5.87; N, 4.63%); m.p. >250 °C (decomp.).

[LaL^3]$^-$: prepared in an analogous manner to the europium complex, ester **2b** (508 mg, 0.472 mmol) being subjected to base hydrolysis, followed by reaction with lanthanum acetate (166 mg, 0.524 mmol); preparative HPLC (t_R = 9.2 min) afforded a white solid (130 mg, 25%); δ_H(D$_2$O, pD $\approx$6) 2.14 (4 H, d, J = 15, CH$_2$), 2.30 (8 H, d, J = 12 Hz, CH$_2$), 3.0–3.6 (20 H, br m, CH$_2$), 3.72 (12 H, s, OMe), 6.8 (12 H, br m, aryl H) and 7.21 (4 H, t, aryl H); δ_P(pD 6) 37.5 and 38.8 (ratio $\approx$8:1) (collapsed to a singlet on heating); $\tilde{\nu}_{max}$(KBr disc) 3135, 3049, 1762, 1601, 1405, 1261 and 1163 cm^{-1}; negative-ion electrospray mass spectrum: m/z 1099.24 (C$_{44}$H$_{60}$LaN$_4$O$_{12}$P$_4$ requires 1099.22); m.p. >250 °C (decomp.).

[H$_3$O][TbL^4]: δ_P(D$_2$O) 521 (br); negative-ion electrospray mass spectrum: m/z 1119.3, 1120.3 and 1121.3 (C$_{44}$H$_{60}$N$_4$O$_{12}$P$_4$Tb requires 1119.24).

[H$_3$O][EuL^4]: δ_P(D$_2$O) 84.6; negative-ion electrospray mass spectrum: m/z 1111.3, 1113.2 and 1114.2.

[H$_3$O][GdL^4]: negative-ion electrospray mass spectrum: m/z 1115.3, 1116.3, 1117.3, 1118.39, 1119.6, 1120.4 and 1121.4.

References

1 G. Mathis, *Clin. Chem.*, 1995, **41**, 1391; 1993, **39**, 1953.
2 E. Soini, L. Hemmila and P. Dhalen, *Am. Biol. Clin.*, 1990, **48**, 567; N. Sabbatini, M. Guardigli and J.-M. Lehn, *Coord. Chem. Rev.*, 1993, **123**, 201.
3 R. A. Evangelista, A. Pollak, B. Allore, E. F. Templeton, R. C. Moiton and E. P. Diamandis, *Clin. Biochem.*, 1988, **21**, 173; E. F. G. Dickson, A. Pollak and E. P. Diamandis, *J. Photochem. Photobiol. B. Biol.*, 1995, **27**, 3.
4 J. Coates, P. G. Sammes and R. M. West, *J. Chem. Soc., Chem. Commun.*, 1995, 1107.
5 P. R. Selvin, T. M. Rana and J. E. Hearst, *J. Am. Chem. Soc*, 1994, **116**, 6029.
6 R. B. Lauffer, *Chem. Rev.*, 1987, **87**, 901.
7 K. Kumar and M. F. Tweedle, *Pure Appl. Chem.*, 1993, **65**, 515.
8 D. H. Powell, M. Favre, N. Graeppi, O. M. Ni Dhubghaill, D. Pubanz and A. E. Merbach, *J. Alloys Compounds*, 1995, **255**, 246.
9 S. Aime, M. Botta, M. Fasano, S. G. Crich and E. Terreno, *J. Bioinorg. Chem.*, 1996, **1**, 312.
10 R. Hazama, K. Umakoski, C. Kabuto and Y. Sasaki, *Chem. Commun.*, 1996, 15.

11 D. Parker and J. A. G. Williams, *J. Chem. Soc., Dalton Trans.*, 1996, 3613; P. K. Pulukkody, T. J. Norman, D. Parker, L. Royle and C. J. Broan, *J. Chem. Soc., Perkin Trans. 2*, 1993, 605.

12 A. Harrison, C. A. Walker, K. A. Pereira, D. Parker, L. Royle, K. Pulukkody and T. J. Norman, *Magn. Reson. Imaging*, 1993, **11**, 761.

13 S. Aime, M. Botta, D. Parker and J. A. G. Williams, *J. Chem. Soc., Dalton Trans.*, 1996, 17; S. Aime, M. Botta, D. Parker and J. A. G. Williams, *J. Chem. Soc., Dalton Trans.*, 1995, 2259.

14 S. Aime, A. S. Batsanov, M. Botta, J. A. K. Howard, D. Parker, K. Senanayake and J. A. G. Williams, *Inorg. Chem.*, 1994, **33**, 4696.

15 D. Parker and J. A. G. Williams, *J. Chem. Soc., Perkin Trans. 2*, 1996, 1581; A. Beeby, D. Parker and J. A. G. Williams, *J. Chem. Soc., Perkin Trans. 2*, 1996, 1565; D. Parker and J. A. G. Williams, *J. Chem. Soc., Perkin Trans. 2*, 1995, 1305; M. Murru, D. Parker, J. A. G. Williams and A. Beeby, *J. Chem. Soc., Chem. Commun.*, 1993, 1116.

16 A. Beeby, R. S. Dickins, S. Faulkner, D. Parker and J. A. G. Williams, *Chem. Commun.*, 1997, 1401.

17 W. B. Lewis, J. A. Jackson, J. F. Lemons and H. Taube, *J. Chem. Phys.*, 1963, **36**, 694; H. Donato and R. B. Martin, *J. Am. Chem. Soc.*, 1972, **94**, 4129.

18 E. Cole, R. C. B. Copley, J. A. K. Howard, D. Parker, G. Ferguson, J. F. Gallagher, B. Kaitner, A. Harrison and L. Royle, *J. Chem. Soc., Dalton Trans.*, 1994, 1619.

19 S. Aime, M. Botta and G. Ermondi, *Inorg. Chem.*, 1992, **32**, 4296.

20 C. D. Klaassen and J. B. Watkins III, *Pharmacol. Rev.*, 1984, **36**, 1.

21 C. J. Broan, J. P. L. Cox, A. S. Craig, R. Kataky, D. Parker, A. Harrison, A. M. Randall and G. Ferguson, *J. Chem. Soc., Perkin Trans. 2*, 1991, 87; P. Wedeking, K. Kumar and M. F. Tweedle, *Magn. Reson. Imaging*, 1992, **10**, 641.

22 P. J. Bohdiewicz, D. K. Lavallee, R. A. Fawwaz, J. H. Neuhouse, S. F. Oluwofe and P. O. Alderson, *Invest. Radiol.*, 1990, **25**, 765 and refs. therein.

23 D. Parker, *Chem. Br.*, 1994, 833.

24 A. Abusaleh and C. F. Meares, *Photochem. Photobiol. A*, 1984, **39**, 763.

25 W. DeW. Horrocks, jun. and D. R. Sudnick, *Acc. Chem. Res.*, 1981, **14**, 384.

26 R. S. Dickins, D. Parker, A. S. de Sousa and J. A. G. Williams, *Chem. Commun.*, 1996, 697.

27 I. Bertini, P. Turano and A. J. Vila, *Chem. Rev.*, 1993, **93**, 2833.

28 C. N. Reilley, B. W. Good and J. F. Desreux, *Anal. Chem.*, 1975, **47**, 2110.

29 B. Bleaney, *J. Magn. Reson.*, 1972, **8**, 91.

30 B. Bleaney, C. M. Dobson, B. A. Levine, R. B. Martin, R. J. P. Williams and A. V. Xavier, *J. Chem. Soc., Chem. Commun.*, 1992, 791.

31 C. N. Reilley, B. W. Good and R. D. Allendoerfer, *Anal. Chem.*, 1976, **48**, 1446; M. D. Kemple, B. D. Ray, K. B. Lipkowitz, F. G. Prendergast and B. D. N. Rao, *J. Am. Chem. Soc.*, 1988, **110**, 8275.

32 J. A. Peters, *J. Magn. Reson.*, 1986, **68**, 240.

33 (*a*) G. M. Sheldrick, SHELXTL, Version 5/VMS, Siemens Analytical X-ray Instruments, Madison, WI, 1995; (*b*) SADABS, Empirical Absorption Corrections Program, University of Göttingen, 1997.

34 Y. Haas and G. Stein, *J. Chem. Phys.*, 1971, **75**, 3668; see also K. Nakamura, *Bull. Chem. Soc. Jpn.*, 1982, **55**, 2697; S. R. Meech and D. Phillips, *J. Photochem.*, 1983, **23**, 193.

35 A. Harrison, C. A. Walker, K. A. Pereira, L. Royle, D. Parker, R. C. Matthews and A. S. Craig, *Nucl. Med. Commun.*, 1992, **13**, 667.

36 T. J. Norman, D. Parker, F. C. Smith, A. Harrison, L. Royle and C. Walker, *Supramol. Chem.*, 1995, **4**, 305.